DESIGN OF AN INVERTED L-C-SHAPE ELECTROMAGNETIC BAND GAP ANTENNA USING SNG MATERIALS FOR C-BAND APPLICATION

By

Brishty Shil

21METE009F

A thesis submitted in partial fulfillment of the requirements for the degree of MASTER of SCIENCE in Electronics and Telecommunication Engineering

Department of Electronics and Telecommunication Engineering

CHITTAGONG UNIVERSITY OF ENGINEERING AND TECHNOLOGY

DECEMBER 2024

Declaration

I hereby declare that the work contained in this Thesis has not been previously submitted to meet the requirements for an award at this or any other higher education institution. To the best of my knowledge and belief, the Thesis contains no material previously published or written by another person except where due reference is cited. Furthermore, the Thesis complies with PLAGIARISM and ACADEMIC INTEGRITY regulation of CUET.

Brishty Shil

21METE009F

Department of Electronics and Telecommunication Engineering

Chittagong University of Engineering & Technology (CUET)

List of Publications

- Shil, B., Das, D., Hossain, M. A., Rahman, M. A., **“**Design of a unique H-L shape EBG Antenna for 5G Telecommunication Technology”,*2024 4th Int. Conf. on Innovations in Science, Engineering and Technology (ICISET)*, Chittagong, Bangladesh,26-27 October 2024, pp 1-6. [Accepted]

- Shil, B., Das, D., Hossain, M. A.,” Design of an Inverted L-C-shape Electromagnetic Band Gap Antenna using ENG Metamaterial for C-Band Application”,*27th International Conference on Computer and Information Technology (ICCIT) 2024*, Cox’s Bazar, Bangladesh, December 20-22, 2024, pp 1-6. [Accepted]
- Shil, B., Das, D., M. H. R., Hossain, M. A.,” Design and Characterization Analysis of C-shape Unit Cell for Wideband Communication Systems”,*27th International Conference on Computer and Information Technology (ICCIT) 2024* Cox’s Bazar, Bangladesh, December 20-22, 2024, pp 1-6. [Accepted]

Approval/Declaration by the Supervisor(s)

This is to certify that Brishty Shil has carried out this research work under my supervision and that she has fulfilled the relevant Academic Ordinance of the Chittagong University of Engineering and Technology so that she is qualified to submit the following Thesis in the application for the degree of MASTER of SCIENCE in Electronics and Telecommunication Engineering. Furthermore, the Thesis complies with the PLAGIARISM and ACADEMIC INTEGRITY regulations of CUET.

Dr. Md. Azad Hossain

Professor

Department of Electronics and Telecommunication Engineering

Chittagong University of Engineering & Technology

Acknowledgement

All praises and thanks to Almighty and the Most Merciful for helping me to accomplish this work. I am grateful to Almighty for giving me good health and well-being. I wish to express my sincere gratitude to Dr. Md. Azad Hossain, supervisor of my thesis, Professor & Head of the Department of Electronics and Telecommunication Engineering, for providing me necessary facilities for the research.

I am also grateful to my parents, family members, and friends for their love, morals, continuous encouragement, and unwavering support in my whole journey.

Abstract

An Inverted L-C-shape EBG antenna is presented for C-band application in communication technology in this thesis. An Epsilon Negative (ENG) Material is used for an effective antenna design.FR-4 material is used as a substrate of 11×11 mm^2 dimensions in this design having a dielectric constant is 4.3 and a thickness is 1.6 mm in unit cell design. But the dimension of the antenna is double to unit cell dimensions such as 22×22 mm^2 where the main patch antenna, EBG structure, or unit cell design consists of copper metal with 0.035 mm thickness and 10×10 mm^2 dimension. At the resonant frequency of 8.01 GHz, the return loss magnitude is -42.29 dB for the proposed EBG antenna and covers the C-band and lower ling of X-band quality to communicate. A 90.0 MHz bandwidth was obtained from the inverted L-C-shape EBG antenna. Instead, the conventional microstrip patch antenna provides 60 MHz bandwidth at the resonant frequency of 7.11 GHz. The gain and directivity of the proposed EBG antenna are 6.42 dBi and 7.27 dBi. Similarly, the required SNG material provides the only negative value of electric polarizability is -1.69 enclosing the C-Band at the resonant frequency of 7.11 GHz. The efficiency rate is 68.52% which refers to good EBG antenna performance. The resulting performance with EBG technology provides better performance such as return loss, far-field directivity, and bandwidth than a basic microstrip patch antenna (without EBG). Specifically, the utilizing properties of electromagnetic waves of ENG materials provides strengthening gain and overall performance in EBG Antenna technology and that's the goal of our thesis study.

বিমূর্ত

এই থিসিসে যোগাযোগ প্রযুক্তিতে সি-ব্যান্ড অ্যাপ্লিকেশনের জন্য একটি উল্টানো এল-সি-আকৃতির ইবিজি অ্যান্টেনা উপস্থাপন করা হয়েছে। একটি এপসিলন নেগেটিভ (ENG) উপাদান একটি কার্যকর অ্যান্টেনা ডিজাইনের জন্য ব্যবহার করা হয়। FR-4 উপাদানটি 11×11 mm2 মাত্রার একটি সাবস্ট্রেট হিসাবে ব্যবহার করা হয় এই ডিজাইনে একটি ডাইলেক্ট্রিক ধ্রুবক 4.3 এবং ইউনিট সেল ডিজাইনে একটি পুরুত্ব 1.6 মিমি। কিন্তু অ্যান্টেনার মাত্রা একক কোষের মাত্রার দ্বিগুণ যেমন 22×22 mm2 যেখানে প্রধান প্যাচ অ্যান্টেনা, EBG কাঠামো বা ইউনিট সেল ডিজাইনে 0.035 মিমি পুরুত্ব এবং 10×10 মিমি 2 মাত্রা সহ তামা ধাতু থাকে। 8.01 GHz এর রেজোন্যান্ট ফ্রিকোয়েন্সিতে, প্রস্তাবিত EBG অ্যান্টেনার জন্য রিটার্ন ক্ষতির মাত্রা -42.29 dB এবং যোগাযোগের জন্য C-ব্যান্ড এবং X-ব্যান্ডের নিম্ন লিং কে গুণমানকে কভার করে। একটি 90.0 MHz ব্যান্ডউইথ উল্টানো L-C- আকৃতির EBG অ্যান্টেনা থেকে প্রাপ্ত হয়েছিল। পরিবর্তে, প্রচলিত মাইক্রোস্ট্রিপ প্যাচ অ্যান্টেনা 7.11 GHz এর রেজোন্যান্ট ফ্রিকোয়েন্সিতে 60 MHz ব্যান্ডউইথ প্রদান করে। প্রস্তাবিত EBG অ্যান্টেনার লাভ এবং ডিরেক্টিভিটি হল 6.42 dBi এবং 7.27 dBi। একইভাবে, প্রয়োজনীয় এসএনজি উপাদান বৈদ্যুতিক মেরুকরণের একমাত্র নেতিবাচক মান প্রদান করে -1.69 সি-ব্যান্ডকে 7.11 গিগাহার্জের অনুরণিত ফ্রিকোয়েন্সিতে ঘেরা। দক্ষতার হার হল 68.52% যা ভাল EBG অ্যান্টেনার কার্যকারিতা বোঝায়। EBG প্রযুক্তির সাথে ফলস্বরূপ পারফরম্যান্স একটি বেসিক মাইক্রোস্ট্রিপ প্যাচ অ্যান্টেনার (EBG ছাড়া) তুলনায় রিটার্ন লস, দূর-ক্ষেত্রের দিকনির্দেশনা এবং ব্যান্ডউইথের মতো ভাল কর্মক্ষমতা প্রদান করে। বিশেষভাবে, ENG উপকরণের ইলেক্ট্রোম্যাগনেটিক তরঙ্গের ব্যবহার বৈশিষ্ট্যগুলি EBG অ্যান্টেনা প্রযুক্তিতে শক্তিশালী লাভ এবং সামগ্রিক কর্মক্ষমতা প্রদান করে এবং এটিই আমাদের থিসিস অধ্যয়নের লক্ষ্য।

Table of Contents

List of Figures

List of Tables

Table No. **Table Caption** **Page No.**

Chapter 1: INTRODUCTION

1.1 BACKGROUND

The electromagnetic band gap characteristics of metamaterials are a kind of novel gift to the world of material science such as the application of EBG antenna. The mode of electromagnetic waves serves to improve the overall performance of the antenna technology at a certain frequency. However, Metamaterials (MTMs) possess remarkable periodic structures and electromagnetic wave properties. It is also represented as a three-dimensional pattern in the entire design. When more than one cell is stated together in a symmetrical system or periodic structure, it refers to the cell array. The array structure also provides the properties of epsilon negative and mu negative behavior to allocate the transmitting signal in this study. So, to develop a material with finer performance the unit cell is important for its smallest periodic structures. Metallic or silvery elements usually refer to the construct of the ground plane where the electromagnetic band gap cell is stored periodically [1]. In the world of electromagnetic, antenna, or microwave systems, the concept of electromagnetic band gap is stated for periodic structures, and the analytical method of Finite Difference Time Domain is discussed [2]. Also, to improve the capability of antenna technology or microwave applications, the metamaterials provide outstanding performance using the properties of Single Negative (SNG) or Double Negative (DNG) metamaterials.

Due to the electromagnetic wave characteristics of the metamaterial, we proposed an EBG antenna that originated for our research purpose, which was demonstrated step by step in the following section. Particularly, the negative of permittivity refers to Epsilon Negative Materials (ENG). The material types also refer to Single Negative (SNG) Materials. It has many applications such as antenna technology, absorbers, sensor-related applications, clocking applications, and radio transmission systems. Other benefits of low profile or size reduction stability are found in this EBG Antenna technology without disturbance. The ability of proper electric line flow through the materials was observed by these Epsilon negative materials. So, in communication systems, multiband materials or an array of materials are used to optimize gain or the outcomes of systems [3]. Also, EBG antenna are used in microwave frequency range or broader distance types communication systems or cell phones very smartly. Nowadays, the EBG structures or meta surface structures used to improve the performance of circularly polarized microstrip patch antenna. So, by using these electromagnetic properties, size reduction may occur in the antenna and is applicable to the microwave frequency range. These band gap behaviors are used in artificial intelligence technology based on sensors or clocking and signals in the communication section. The efficiency of the trunks of receiving transmitter power may increase by the electromagnetic properties of EBG structures. For X-band satellite transceiver applications, a woodpile EBG structure was designed and optimized for the development of gain in antenna technology. However, the EBG concept may increase the communication systems.

In this thesis, a novel unit cell is designed and optimized for the properties of the metamaterials. Particularly, the negative of permittivity refers to Epsilon Negative Materials (ENG). So the resulting properties refer to the Epsilon Negative (ENG) Materials and cover the C-band and X-band frequency range. The material types also refer to Single Negative (SNG) Materials. It has a wide range of applications such as antenna technology, absorber, sensor-related applications, and radio transmission system, However, At the resonant frequency of 8.01 GHz, the return loss magnitude is -42.29 dB (FR-4) for the proposed EBG antenna and covers the C-band quality to communicate. Due to the electromagnetic wave characteristics of this metamaterial, the proposed EBG antenna originated in our research purpose and was demonstrated step by step in the following section. Due to the size reduction of the patch dimension and proper impedance matching this EBG antenna is resonant at 8.01 GHz. So it reminds the better-reflected electromagnetic waves found without any disturbance in our proposed Inverted L-C-shape EBG design for its higher magnitude of return loss performance.

In telecommunication systems, frequency bands offer to allow or transmit the signal without disturbance. C-band and X-band hold the frequency range from 4 GHz to 12 GHz. C-band offers cheaper bandwidth significantly broader range of transmitting systems. For satellite communication technology, the C-band is used to increase and cover 5G networks. The C-band is also able to assist the 5G tele-networks with wide distances. So the lower and higher range of these bands also provides small-size data transmission at Very Small Aperture Terminal (VAST). Also, the installation system of these is easy and effective for users in any area. Also, satellite application or radars from the ground link (3GHz- 4GHz) to the upper link(5GHz to 6GHz) provides a wider range of transmitting and receiving systems. And X-band offers a cost-effective device, especially for making small antenna. So that it may use various applications frequently on higher power systems. Similarly, the C-band offers a small-size antenna design depending on the wavelength in antenna technology. The disadvantages of having C-band and X-band focused on maintenance, cost, and size of the antenna. However, the limitations of these bands may be overcome by their significant features and applications. By inspiring the previous research work and overcoming the limitation of metamaterials science and antenna technology, this thesis work proposed better outcomes. Our proposed unit cell and arrays both are enable to cover C-band and X-band. Additionally, the proposed EBG antenna holds these bands by its electromagnetic band gap properties.

1.2 PROBLEM STATEMENT

To achieve peak success in material science or communication systems proper behavior of metamaterials is important. In this thesis, a unique unit cell may be designed and optimized with good performance for constructing a strengthening electromagnetic band gap type antenna. Sometimes, it's difficult to make desirable antenna designs for large-size conditions. Fortunately, this electromagnetic band gap-type antenna provides simplicity of design and size. Designers or researchers may develop their skills in this section.

The SNG materials are found in nature and that's a great advantage of transmitting or communication-based applications. Stepwise evaluation of the design will be designed by good observation for processing of transmitting signal. Similarly, the ability to approach the transmitting system at low or high frequencies provides a good response for designing the desired system. So, the study of this thesis focuses on the development and enhanced performance of EBG Antenna.

1.3 AIMS AND OBJECTIVES

The utilizing properties of electromagnetic waves of a Single Negative Materials provide strengthening performance in electromagnetic band gap antenna technology and that's the goal of our thesis. To enhance the overall performance of antenna technology the concept of an EBG unit cell differs from other techniques and offers various types of applications in a certain frequency for any wireless communication system.

The main objectives of this thesis are as follows:

- To design and analyze the properties of a unit cell for recognition as an SNG metamaterial.
- To evaluate the performance of the array unit cell of the metamaterial for dual bad application and the performance parameter of the EBG antenna.

1.4 SIGNIFICANCE, SCOPE, AND DEFINITIONS

An Inverted L-C-shape EBG antenna is presented for C-band application in this thesis. Microstrip line feeding method used to transmitting power in this design. Also, the characteristics of this proposed unit cell are optimized to clarify the specific metamaterial types of SNG materials based on the Finite Integration Technique (FIT). To develop the enhanced quality of the proposed EBG antenna, the conventional microstrip patch antenna is also designed and compared with the EBG antenna.

Generally, an Antenna refers to an electrical device that converts electric power into electromagnetic waves or converts electrons to photons. the antenna radiates the energy from the current as electromagnetic waves (radio waves).

Electromagnetic band gap structures consist of periodic metal patches on a dielectric substrate. That creates a stopband to block electromagnetic waves of certain frequency bands. So, the proposed antenna provides outstanding performance parameters in this thesis which also balances the frequency band in EBG antenna technology. In a communication system, the proposed unit cell will also be used in an absorber, sensor, or integrated circuit system. Hence, systematic materials always supply goods application in the communication system without any trouble. So, EBG Antenna ensures the enhanced quality of gain, directivity, and return loss performance at the required frequency of 8 GHz.

1.5 THESIS OUTLINE

Chapter 2 reviews the literature background of metamaterials and their types. Also, discuss previous work of EBG Antenna and the proposed antenna.

Chapter 3 focuses on the proposed design of the metamaterial and its characteristics. Stepwise design evaluation explained with essential parameters. Unit Cell Array structure is developed and explained in this section. Analysis of the array properties.

Chapter 4 contains the design of the microstrip patch antenna. The proposed EBG antenna with specifications is also described in this section.

Chapter 5 describes the overall performance of the EBG antenna compared with the microstrip patch antenna.

Chapter 6 is the conclusion section of the overall performance of the proposed EBG Antenna in communication technology and future outcomes in antenna technology.

Chapter 2: LITERATURE REVIEW

2.1 BACKGROUND AND METAMATERIALS

From the Greek word 'meta', the word Metamaterials is established. Metamaterials are arranged based on the magnitude (negative or positive) of these material's properties. However, Metamaterials are artificial substances that behave in ways not found in substances in the natural world.Using this property of negative permittivity or permeability, both are in negative magnitude, the metamaterials provide excellent advantages for communication systems. The properties of epsilon negative and mu negative materials will be obtained by having higher bandwidth and gain of the cell systems. The capability of absorption will be observed in this study which is a significant advantage of wireless communication systems or sensing applications. Negative Refractive Index (NRI) behavior was first observed in Smith's studies where loop wiring and Split Ring Resonators (SRRs) were used to acknowledge the behavior [4]. This behavior also provides left-handed characteristics [5]. Single negative characteristics are also used to identify the left-handed materials [6]. Various types of applications may develop by this concept of electromagnetic waves. Similarly, different shapes of materials were developed using the concept of SNG or DNG characteristics. In communication systems, multiband materials or an array of materials are used to optimize gain or the outcomes of systems [7]. Using the substrate Rogers RT5880, the triple resonant frequency was observed in the sensing application [8]. Triple-band absorbers are also made with electromagnetic compatibility [9]. To improve the capability of antenna technology or microwave applications, the metamaterials provide outstanding performance using the properties of SNG or DNG. For single-band applications, square SRR-shape unit cells are used with NRI properties [10]. The S-band, C-band, and X-band frequencies were obtained for satellite and radar communication [11]. A Z-shape unit cell designed to cover dual band applications with LHM properties [12]. An Epsilon Negative (ENG) material is also used for satellite communication [13]. Various types of unit cells use microwave frequency range in communication systems day by day [14]. Therefore, the characteristics of the unit cell may balance the band frequency very smartly in wideband communication systems. The uses of the electric effect and the force of the magnetic effect are becoming wider day by day in this advanced technology.Also, in multiband applications strong shifting or filtering is important to demonstrate any metamaterials design. For satellite applications such as TV networks or radio communication networks, the meta-atom provides faster networking systems in the microwave range [43]. Similarly, various types of sensor applications or super-lens are made based on the metamaterial property [44]. The uses of material increased widely so a researcher or designer may improve the parameters of material to make any desirable system. As a result, unique or novel metamaterial may be included in material science or communication systems.

2.2 TYPES OF METAMATERIALS

However, types of metamaterials vary by their material properties such as permeability, permittivity, and refractive index. Generally, the ratio of the permittivity of the materials to the permittivity of free space(vacuum) refers to the relative permittivity of the materials. This property also affects the propagation of electric fields so it's an important parameter for electromagnetics applications. At the same time, permeability offers the ability to allow the density of magnetic flux.

If the value of permittivity (ε) or permeability (μ) is negative then it is referred to as Single Negative Materials (SNG). When both are in negative magnitude then it relates to Double Negative Materials (DNG) with negative refractive index [15]. Similarly, the Mu Negative (MNG) materials refer to when the material's properties such as permeability are less than zero ($\mu < 0$) and permittivity is greater than zero ($\varepsilon > 0$). But when the material's oppositive properties of Mu Negative materials then it refers to Epsilon Negative materials such as the permittivity less than zero ($\varepsilon < 0$) and permeability greater than zero ($\mu > 0$). The refractive index changes with the desired frequency in the system for MNG materials and is mostly found in natural materials [16]. However, these four types of metamaterials are represented in Figure 2.1-1.

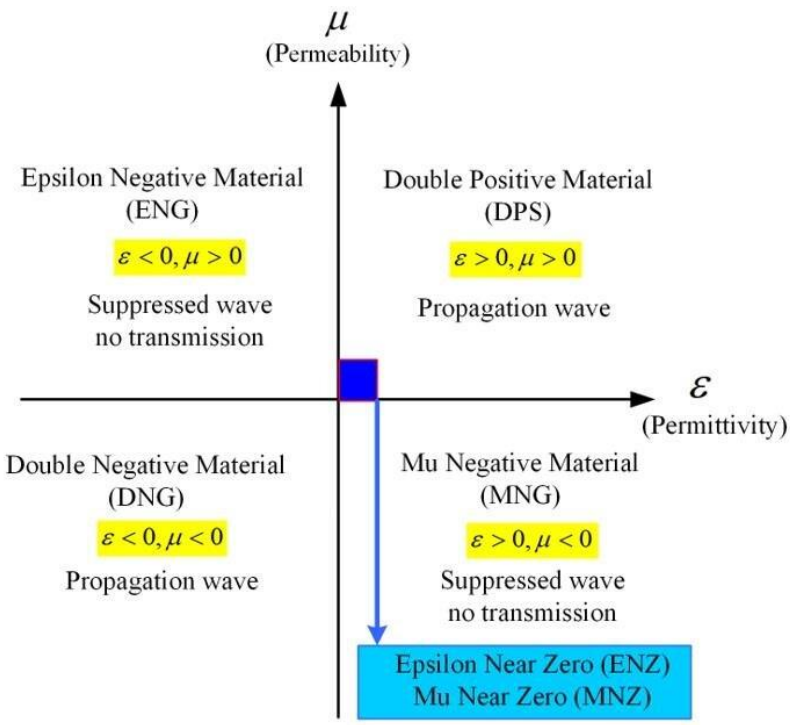

Fig 2.2-1: Types of metamaterials based on permeability and permittivity [16]

2.3 EBG ANTENNA

The mode of electromagnetic waves serves to improve the overall performance of the antenna technology at a certain frequency. The periodic structure of the EBG unit cell differs from all other materials. So, it may induce passband, stopband, or bandgaps and decrease mutual coupling by computing the radiation of electromagnetic waves at a certain frequency. These EBG base periodic materials may not be found in nature so the designer may develop the cell structure depending on interest in any certain frequency range. The EBG crystal or material holds over the ground plane of the desired antenna layout [17]. Metallic or silvery elements usually refer to the construct of the ground plane where the electromagnetic band gap cell is stored periodically. The band diagram also shows the periodic structure and the response of electromagnetic waves [18]. In the world of electromagnetic, antenna, or microwave systems, the concept of EBG is stated for periodic structures, and the analytical method of Finite Difference Time Domain is discussed [19]. The frequency reconfiguring technique works for multiband applications such as wireless communication systems or cell phones [20]. Also, the desired gain and higher bandwidth are other factors for the use of EBG unit cells in antenna technology [21]. To reduce the antenna size provide a dual-band application in wireless telecommunication systems also [22]. However, metamaterial types express both negative permittivity and negative permeability properties that act as double negative material (DNG) [23]. Epsilon-negative materials (ENG) have less than zero permittivity and larger than zero permeability ($\varepsilon < 0$, $\mu > 0$). A Mu negative (MNG) material (permittivity > 0, permeability ≤0) [24]. Using the behavior of DNG materials enhanced the gain of the antenna [25]. Obtained the broader range of multiband or wideband using mushroom EBG [26]. The behavior of controlling electromagnetic waves resulted in higher directivity and bandwidth in EBG antenna technology [27]. Small sizes or size reduction may be caused by EBG slots and obtaining a low-profile EBG antenna [28]. The amplifying quality of electromagnetic waves also provides enhanced gain and is used in small-cell technology [29]. However, the restriction of the antenna design such as lower gain or, insufficient bandwidth may be overcome by using electromagnetic band gap characteristics so it reaches any desired goal at a specific resonant frequency [30]. In a high-speed switching circuit, the electromagnetic band gap offers flexible and smoother signal integrity without noise [31]. Also, ultra-wideband antenna technology, a mushroom-like EBG structure provides accurate band rejection properties [32]. So, the properties of electromagnetic band gap systems are important for creating data connections in a communication network system. In 2018, a modified mushroom-type EBG antenna was designed with a 3.85dB gain performance and covered 72 MHz bandwidth [33]. Using electromagnetic band gap property circular patch antenna designed for 2.45 GHz base application [34].To enhance the gain a four-stacked -T shape EBG structure loaded in antenna technology and provides the return loss is -22 dB [35].In the recent era, To enhance the antenna parameter function the electromagnetic band gap (EBG) technology may be the most recent concept for researchers. So, the improvement of EBG structure increased day by day for antenna technology as well as material sciences and electromagnetics. Slotted-type EBG structure used in antenna design applicable in C-band communication systems [36]. 2.09 dBi gain enhanced by using a rectangular EBG structure in antenna performance for Wi-Fi applications [37]. Also, based on this band gap characteristics C-slot type microstrip patch is designed for WiMAX applications covering 50 Km radius [38]. Size miniaturization is an important factor in choosing good antenna performance. In WiLAN applications, enhancement types EBG slots are used for antenna technology. Hence, the electromagnetic band gap behavior provides this size miniaturization ability to make a low-profile EBG antenna [39]. A low-profile and cost-effective antenna provides desirable outcomes to the communication systems. To achieve better radiation and reduce the side lobe and back side lobe levels the antenna structure is important. The EBG structure loaded on the magnetic ground plane also provides a better radiation pattern and is applicable for wideband communication systems [40]. In planner antenna, the electromagnetic band gap structure is used for various application purposes [41]. However, the dimensions of EBG structures may differ by the periodic crystal structure .So based on the application or systems a researcher may develop the EBG structure for its unique electromagnetic band gap properties.

Chapter 3: UNIT CELL DESIGN METHODOLOGY

3.1 DESIGN APPROACH OF PROPOSED UNIT CELL

To optimize the electromagnetic properties of the proposed unit cell and array design, we need to observe the response of the reflection and transmission coefficient by following equations (1). The properties analysis is applied by Finite Integration Technique (FIT) to measure the scattering parameters.

$$\Gamma = \frac{(z_0 - 1)}{(z_0 + 1)} \quad (1)$$

Here, Γ refers to the reflection coefficient. The relative impedance (Z_0) is determined (2) by

$$z_0 = \sqrt{\frac{\mu_r}{\varepsilon_r}} \quad (2)$$

Also, when the reflection coefficient is obtained definitely at each port it refers to scattering parameters (S-parameters) of the unit cell such as S_{21} and S_{11} [12]. So, the transmittance (S_{21}) and reflectivity (S_{11}) of the unit cell are obtained by the equations of (3) and (4):

$$S_{11} = \frac{(1 - \Gamma^2)z}{1 - \Gamma^2 z^2} \quad (3)$$

$$S_{21} = \frac{(1 - z^2)\Gamma}{1 - \Gamma^2 z^2} \quad (4)$$

The simulated results of the transmittance (S_{21}) and reflectivity (S_{11}) of this proposed unit cell also follow the Nicolson-Ross-Weir (NRW) method and are used to optimize the effective medium characteristics of effective permittivity (ε_r) and permeability (μ_r). Using this method, two composite variables of V_1 and V_2 represent the addition and subtraction of scattering parameters of S_{21} and S_{11} shown in the following equation of (5) and (6),

$$V_1 = S_{21} + S_{11} \quad (5)$$

$$V_2 = S_{21} - S_{11} \quad (6)$$

This equation is also used to separate the effective parameters from $S_{21}$and S_{11}.So, the effective permittivity (ε_r) and permeability (μ_r) determined by the following equation of (7) and (8),

$$\varepsilon_r = \frac{c}{j\pi f d} \times \frac{(1-V_1)}{(1+V_1)} \quad (7)$$

$$\mu_r = \frac{c}{j\pi f d} \times \frac{(1-V_2)}{(1+V_2)} \quad (8)$$

For the effective refractive index, the Direct Refractive method was used to determine this response from the S-parameters of the transmittance (S_{21}) and reflectivity (S_{11}) of the unit cell as follows [45]:

$$\eta_r = \frac{c}{j\pi f d} \times \sqrt{\left\{\frac{(S_{21}-1)^2 - S_{11}^2}{(S_{21}+1)^2 - S_{11}^2}\right\}} \quad (9)$$

Using this mentioned equation the characteristics of the metamaterials found from the analysis of S-parameters and effective permittivity (ε_r), permeability (μ_r) and refractive index (η_r) of the proposed unit cell design. So, the simulated results of real and imaginary values of effective permittivity (ε_r), permeability (μ_r) and refractive index (η_r) may extract from the S-parameters' performance and verify the types of materials explained in the following section.

3.2 METAMATERIAL DESIGN AND RESEARCH WORKFLOW

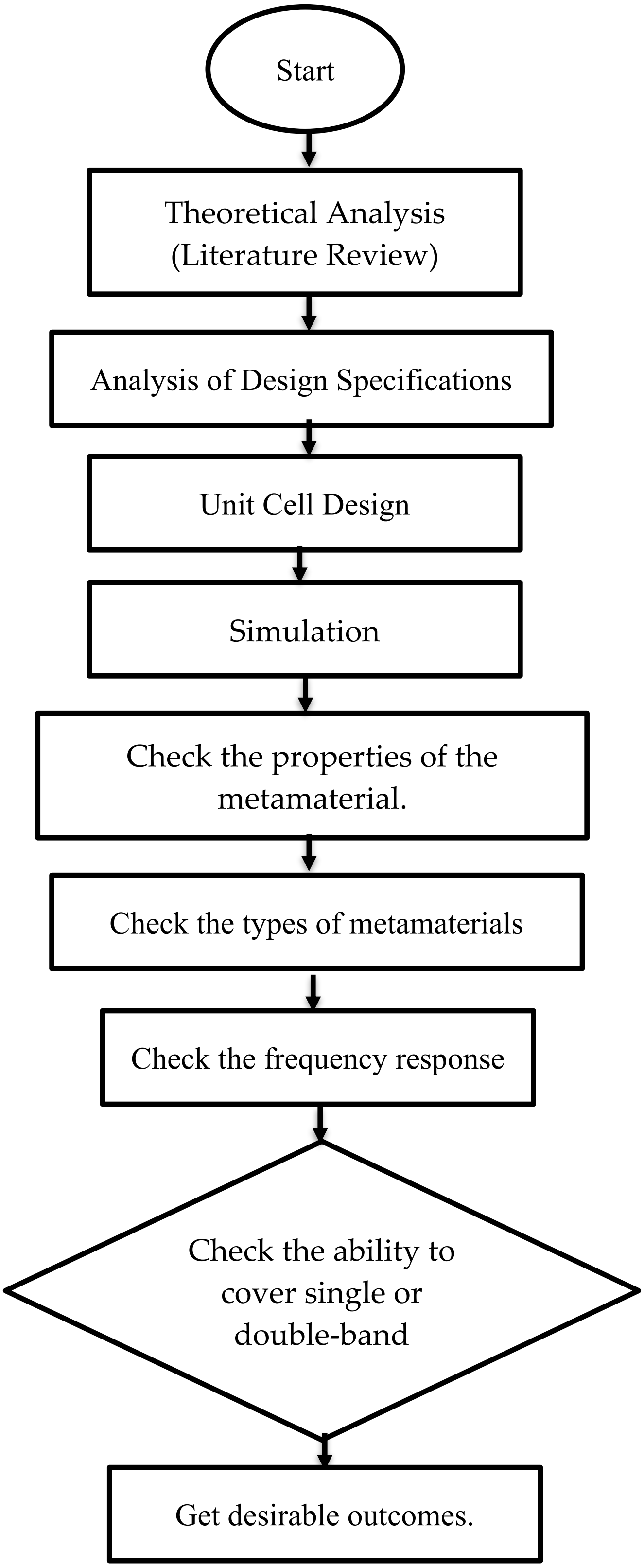

Fig 3.1-1: Flowchart of metamaterials thesis work

3.3 PROPOSED UNIT CELL DESIGN AND SIMULATION SETUP

Substrate selection is important to support any materials design or unit cell type. The metallic elements of the copper split resonator are used to form the metallic structure of the proposed inverted L-C-shape unit cell design in Figure 3.1-2. The copper element is stated on top of the substrate with different sizes of length but the same in width is 0.035 mm. Here, the length and width of square copper metals are c=10 mm and d=10 mm. Rogers RT5880(lossy) substrate materials with a dielectric constant of 2.2 used for overall dimensions of $11\times11\times1.6$ mm^3.Hence, For better performance, we set the thickness of this substrate is 1.60 mm and thermal conductivity is 0.2 $WK^{-1}m^{-1}$. Two L-shape resonators are shaped by copper metal and the width is 1 mm. Also, the width and length of the substrate are the same in dimensions refers the parameter a =11 mm and b= 11mm. Here, the height of copper metal is 0.035 mm declared as Dc, and the height of Rogers substrate is declared as Dr in the design. Different types of square slot gaps were used to obtain better performance of this design as 'g= 0.50 mm' and 'h= 0.75 mm' which are also explained in the following section. Also, we focused on the middle of the structure the cylindrical shape demonstrated by the outer radius of R=1.5 mm and the inner radius is r=1 mm in the proposed design.

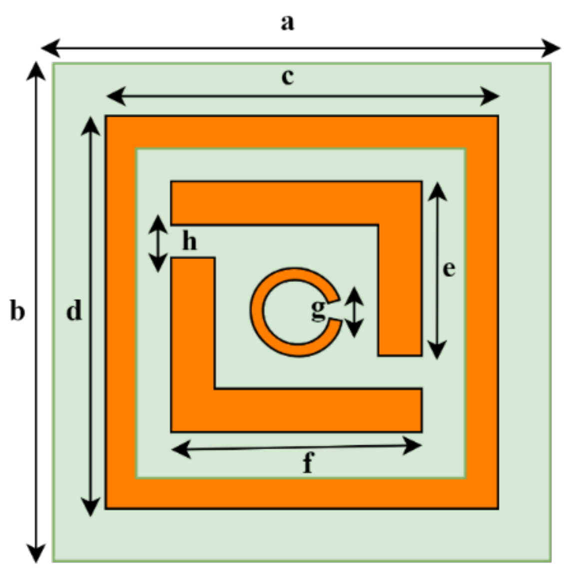

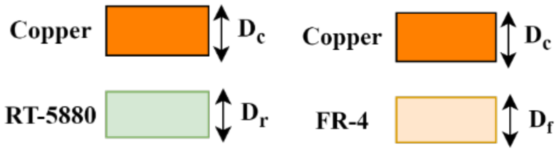

Figure 3.1-2: Geometrical View of Proposed inverted L-C-shape Unit Cell

The properties analysis is applied by Finite Integration Technique (FIT). The proposed unit cell is placed between two waveguide ports such as port-1 and port-2. So transmitting the signal from port-2 to port-1 such as EM wave propagation stated along the positive and negative of the z-axis. The simulation setup is offered by CST Studio Suite software in Figure 3.1-3 which is based on FIT. The CST software provided the way of simulator choice of mesh type as tetrahedral [37]. The magnetic field and electric field are accomplished along with the x-axis and y-axis where the z-axis is executed as an open space in the boundary to control the system. The frequency domain solver is used to minimize the solver runs so it provides fast results in a specific frequency problem.

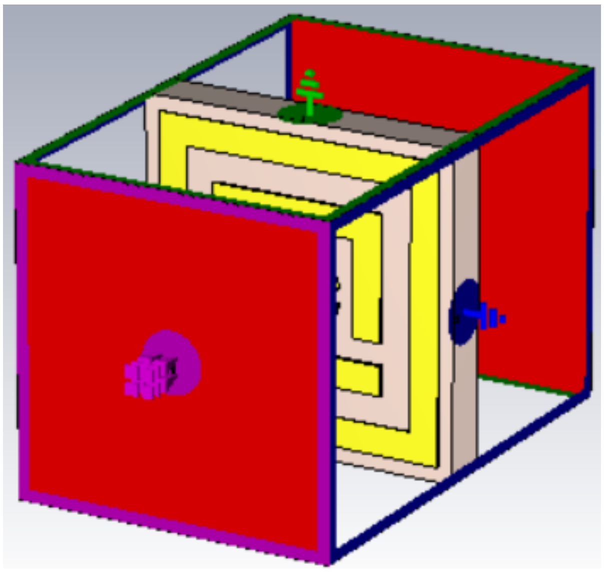

Figure 3.1-3: Simulation setup for proposed unit cell design

3.3.1 Design Specification of Proposed Design

Table 3.1-1 indicates the parametric dimensions unit in millimeters (mm) scale of the proposed design.

Table 3.1-1 Dimension of an inverted L-C-shape unit cell:

Description	Parameters	Value(mm)
Substrate Width	a	11
Substrate Length	b	11
Copper Length	c	10
Copper Width	d	10
Design Parameter	e	4.25
Design Parameter	f	6
Square Gap	g	0.5
Cylindrical Gap	h	0.75

3.3.2 Stepwise Design Workflow Analysis

To reach the required design goal, the stepwise approach of the proposed design is indicated in Figure 3.1-4. The Final step in the diagram focuses on our desired structure. Gradually the outcomes of the transmission coefficient developed in this design and obtained two resonant frequencies indicated by the graphical presentation in Figure 3.1-5. No resonant frequency was found in Step 1. The performance of the transmission coefficient (S_{21}) by changing the step of the offered final design structure. These results indicate the SNG metamaterial properties. The transmission co-efficient reminds the properties of metamaterials such as -70.44 dB of the magnitude of S_{21} indicates the behavior of the unit cell at 7.11 GHz frequency and -37.99 dB of S_{21} mode of transmission at 8.86 GHz frequency whereas the S_{11} is near zero or zero for the system. In Step 1, the magnitude of S_{21} is -5.98 dB at the same frequency of 7.11 GHz. Similarly, the magnitude of S_{21} is -58.54 dB at 7.11 GHz frequency, and the improvement of magnitude from step 2 to the Final proposed step. Hence, the outcomes from the stepwise approach of the Final proposed inverted L-C-shape unit cell cover two frequency bands C-band and X-band, and found the material properties which are also discussed in the result section.

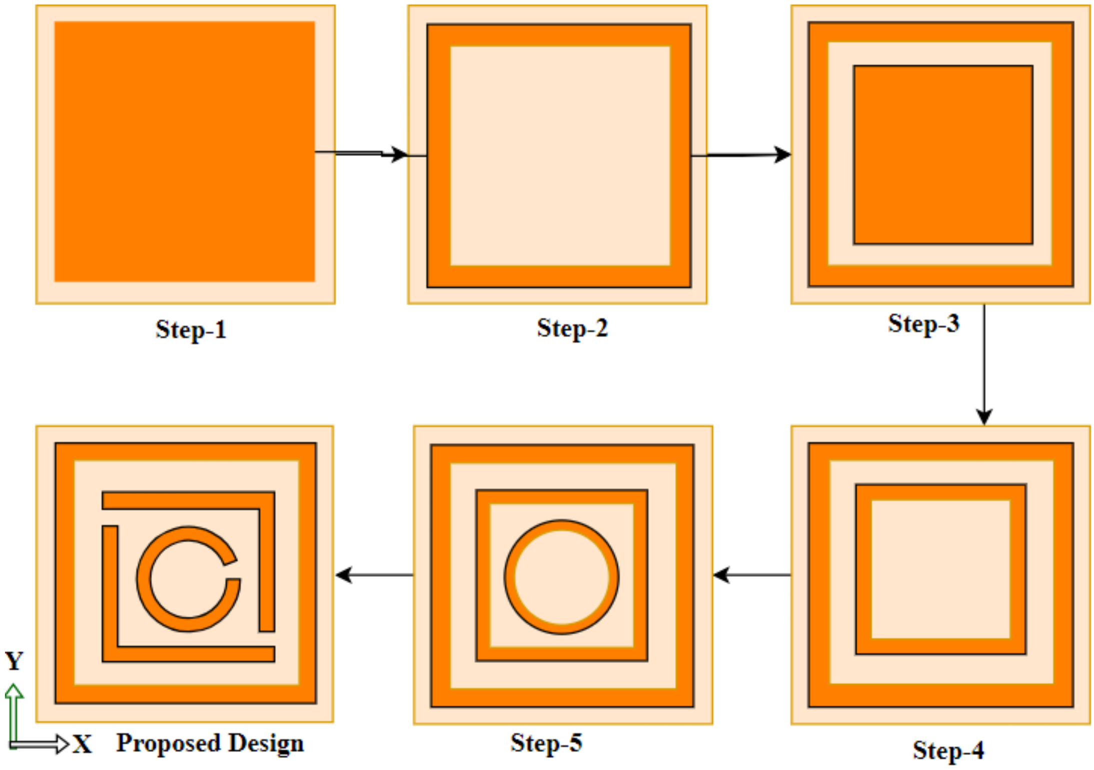

Fig 3.1-4: Stepwise Design Procedure of Proposed Inverted L-C-shape Unit Cell

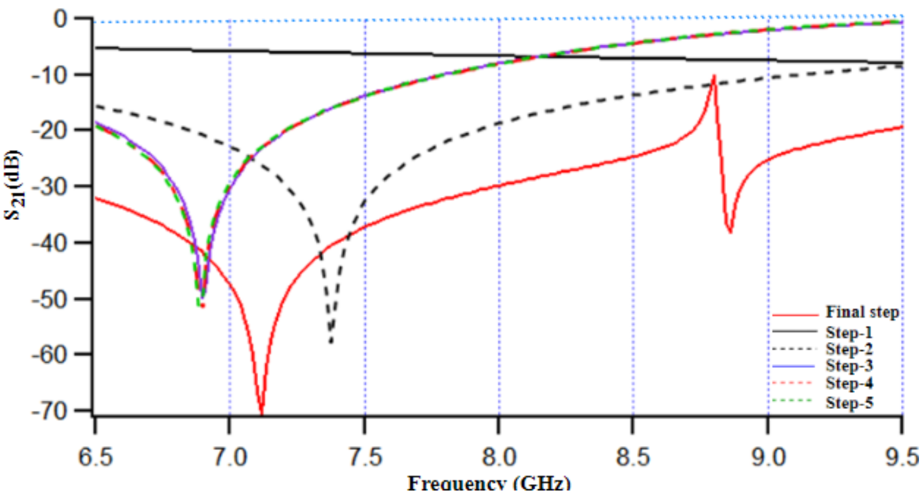

Fig 3.1-5: Stepwise design analysis due to Transmission Co-efficient(S_{21})

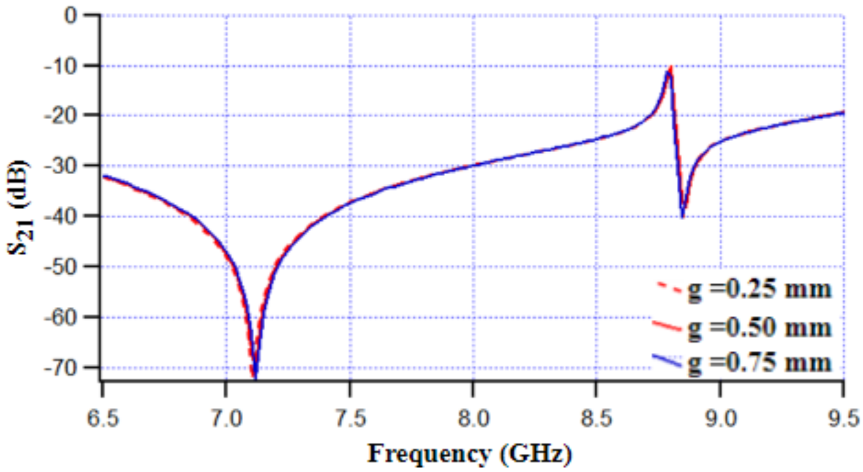

(a)

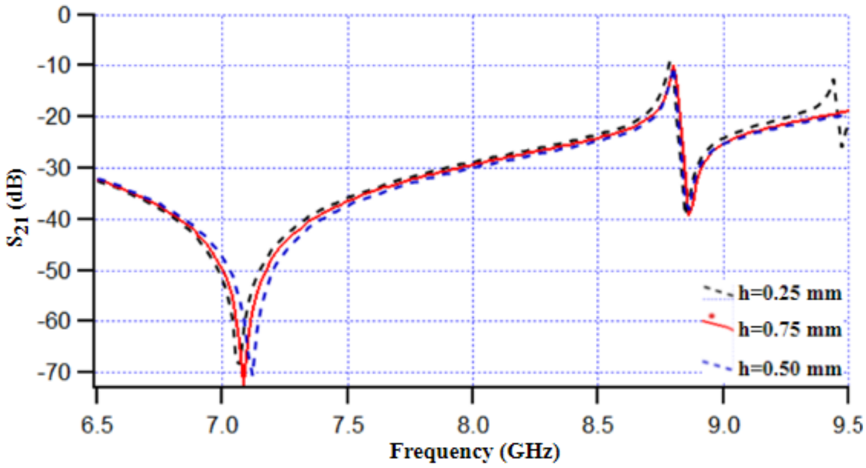

(b)

Fig 3.1-6: Statistics analysis (a) by changing the cylinder gap 'g'(b) by changing the square shape gap 'h'

Figure 3.1-6 indicates the improvement of the magnitude of the transmission coefficient (S_{21}) by changing the cylindrical gap of 'g' and the gap 'h' of the square shape design parameter to reach the desired shape of 'L'. Figure 3.1-6 (a), the cylindrical gap (g) of 0.50 mm offered the desired results at 7.11 GHz and 8.86 GHz frequencies such as -70.44 dB. The change of g = 0.25 mm and g=0.75 mm offered -71.88 dB at the frequency of 7.10 GHz and -72.2 dB at the frequency of 7.12 GHz. Similarly, in Figure 3.1-6 (b) changing the design parameter of h=0.75 mm provided a better magnitude of transmission coefficient in our design such as -72.54 dB at the frequency of 7.11 GHz. Utilizing this two-design parameter we fixed the value of g=0.5 mm and h=0.75 mm offering better magnitude for further analysis and the material properties.

3.3.3 Response of the Proposed Unit Cell

The simulated result of the transmission coefficient and reflection coefficient is shown in Figure 3.1-7. Here, Two resonant frequencies are observed in the proposed unit cell. Two resonant frequencies are induced by electric resonance at 7.11 GHz and 8.86 GHz. The magnitude of the reflection coefficient (S_{11}) is minimum (zero) when the transmission coefficient is maximum in the desired result indicated in this graphical presentation. However, the ratio of the magnitude of transmitted data to incident data refers to the transmission coefficient. So, the probability of transmitting the signal depends on this transmission coefficient. Here, these two resonant points of 7.11 GHz and 8.86 GHz provide material properties of epsilon negative materials (ENG). Similarly, Figure 3.1-8 indicates the response of a) permittivity, b) permeability, and c) refraction index of the proposed materials.

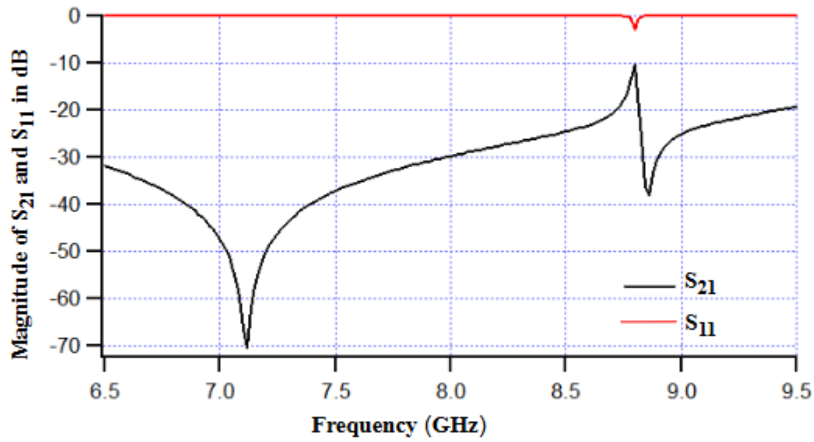

Fig 3.1-7: Response of Transmission Co-efficient (S_{21}) and Reflection co-efficient (S_{11})

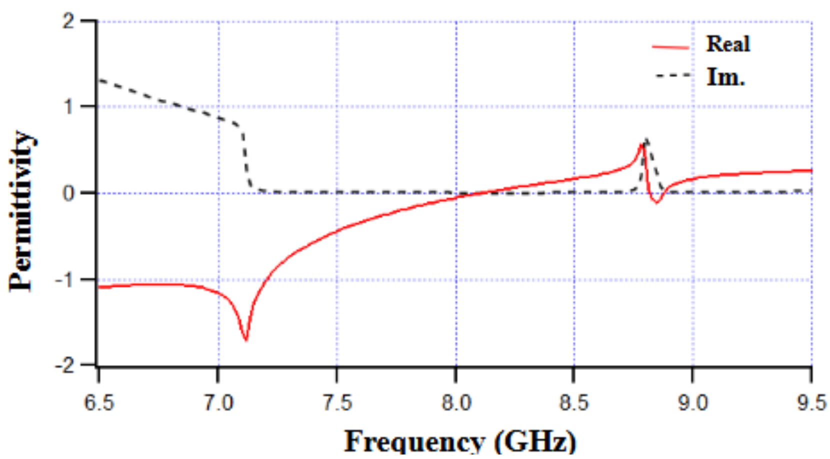

(a)

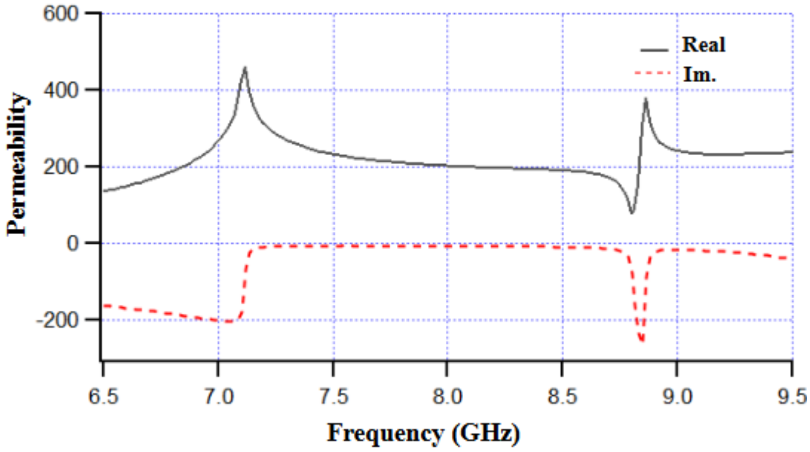

(b)

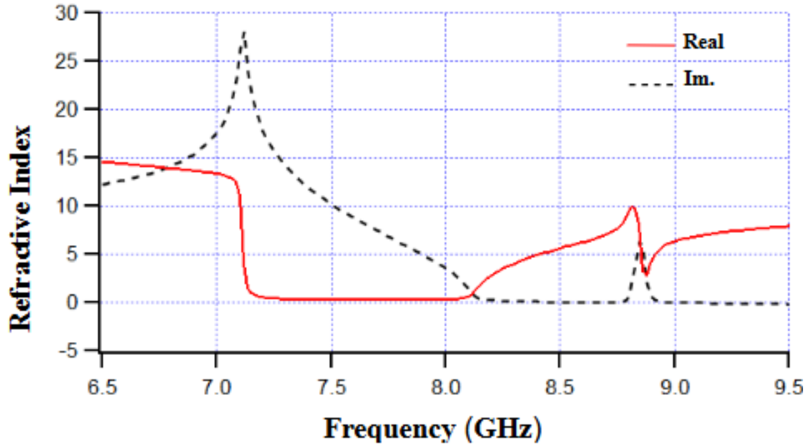

(c)

Figure 3.1-8: Response of (a) Permittivity, (b) permeability, and (c) Refractive index of the proposed design

At the resonant frequencies of 7.11 GHz and 8.86 GHz, the magnitude of permittivity is -1.69 and -0.588 referring to the epsilon negative material in Figure 3.1-7 (a). The refraction index of the proposed design provides a positive magnitude such as 0.83 and 3.02. Balancing the configuration of the design also provides a better response to the properties of epsilon materials. The magnitude of epsilon is less than zero ($\varepsilon < 0$) where the permeability is greater than zero. Hence, the response of the effective medium parameters of this proposed inverted L-C-shape unit cell such as permittivity, permeability, and refraction index refers to the epsilon negative materials property in this study. Figure 3.1-9 (a) indicates the maximum magnitude of the surface current is 180 Am^{-1} to 193 Am^{-1} at the resonant frequencies 7.11 GHz and 8.86 GHz respectively. However, Surface Current Distribution determines the electromagnetic properties of the surface structure.Figure 3.1-9 (b) and Figure 3.1-8 (c) refer to the electric field and magnetic field direction in three-dimensional mode.

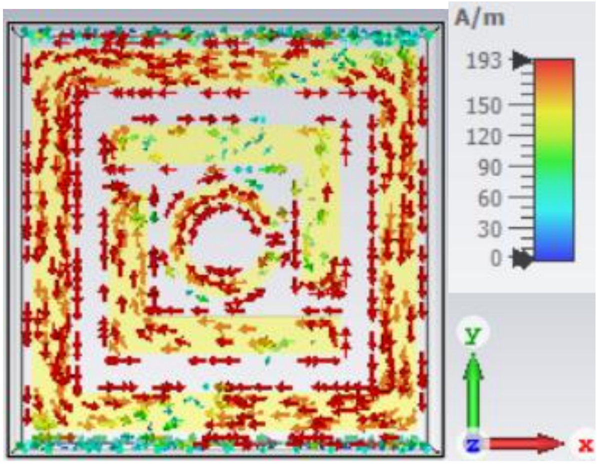

(a)

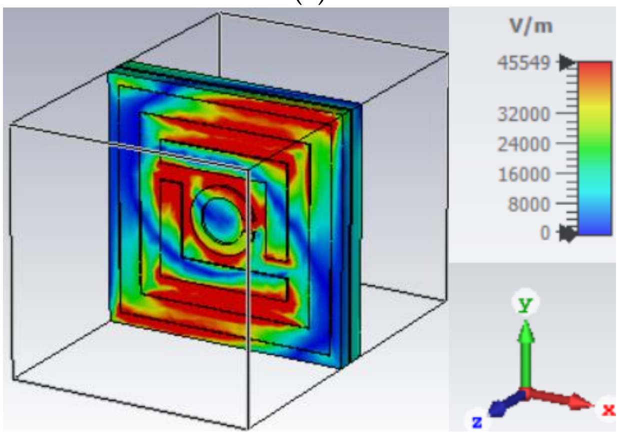

(b)

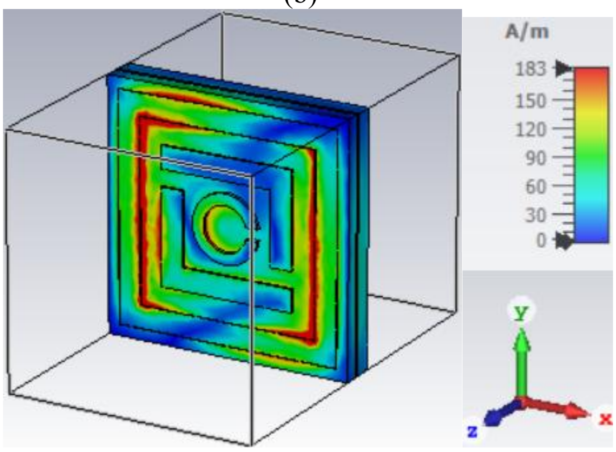

(c)

Fig 3.1-9: Results of (a) Surface Current distribution (b) Electric Field, and (c) Magnetic Field at 7.11 GHz frequency.

3.4 UNIT CELL ARRAY

3.4.1 Two Array Design

To estimate the effect of mutual coupling between unit cells the array structure provides better advantages. Here, Figure 3.2-1 indicates the unit cell array structure (a) 1×2 array and (b) 2×2 array. The dimension of the 1×2 array is 11×22 mm^2 stated on the same substrate of RT5880.In 1×2 array structure p=22 mm and q=11mm denote the width and length of the array structure respectively. Similarly, The width and length of the 2×2 array are s=22 mm and r=22 mm in the design. The thickness of the substrate and copper metal of these two array structures same as the proposed inverted L-C-shape unit cell. The power signal sets the port connection system from port 2 to port 1. The boundary setting of 1×2 array and 2×2 array unit cell is the same as the basic inverted L-C-shape unit cell structure such as the x-axis and z-axis referring to the magnetic and electric fields. Using the array structure, multiple resonant frequencies were obtained to determine the properties of metamaterials which also covered multiple frequency bands in our study. Using a design and analyzed base computer software similar to a proposed unit cell, this two-array structure also provides better performance such as good material properties. The same boundary condition and selection of magnetic field and electric field were applied. Also, the bandwidth of the unit cell array provides a better range for transmitting data in the communication system.

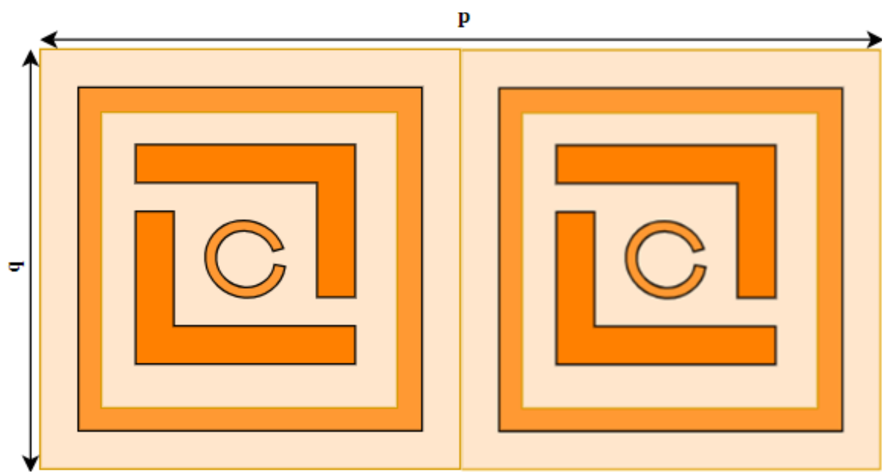

(a)

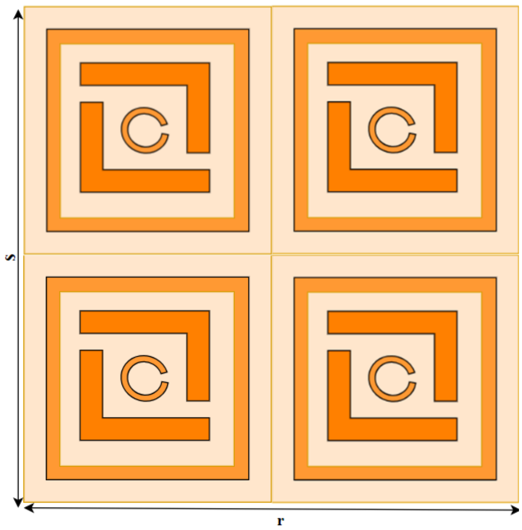

(b)

Fig 3.4-1: Geometrical Unit cell Array Structure (a) 1×2 array (b) 2×2 array

3.4.2 Properties of Array

Here, in a 1×2 array, the cell provides two resonant frequencies. For the effects of electric resonance such as ε are -3.43 and -0.81 indicated in Figure 3.2-2. The 1×2 array cell delivered epsilon negative materials properties in the resonant frequency of 7.15 GHz and 7.82 GHz and covered the C-band frequency band. Hence, the 1×2 array cell balanced the C-band and X-band frequency and is also used for any telecom networking system. However, the 2×2 array cell provides three resonance frequencies indicated in Fig.3.2-2 by the response of materials properties such as permittivity, permeability, and refractive index. Due to electric resonance, there are two operating frequencies 7.15GHz 8.62 GHz, indicating the permittivity is -1.59 and -0.026. According to two this array response for permittivity referred to the epsilon negative materials. This ENG material covers the C and X band frequencies.

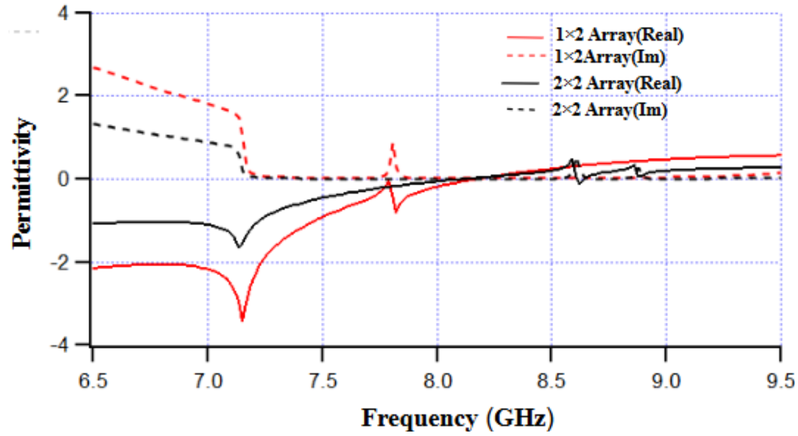

(a)

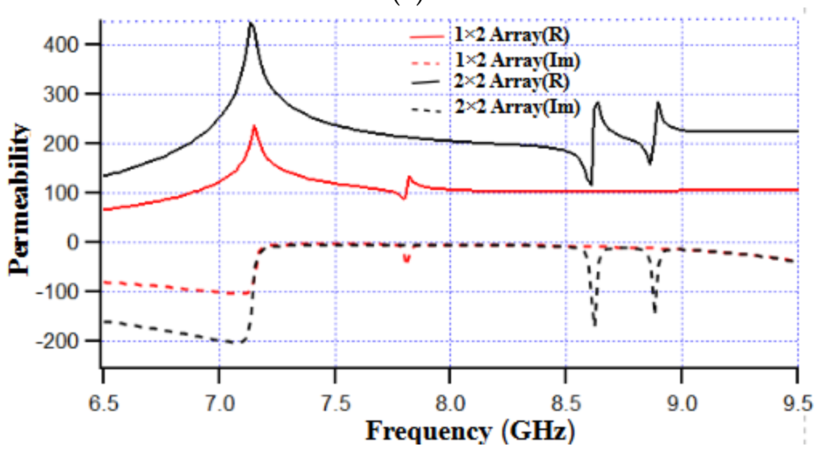

(b)

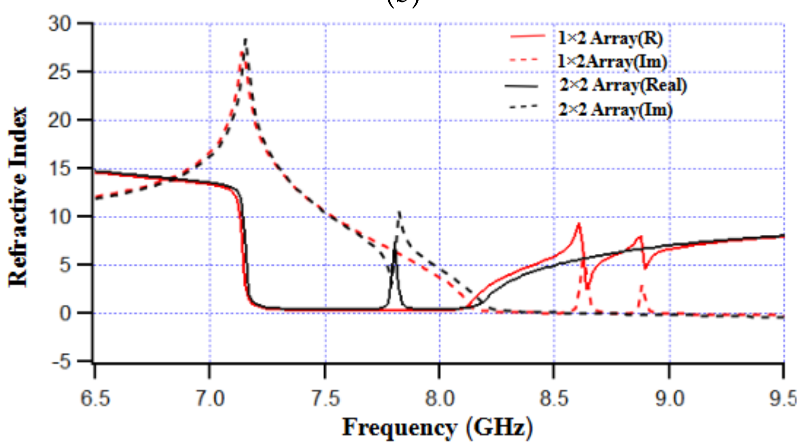

(c)

Fig 3.4-2 Response of the magnitude of 1×2 array cell and 2×2 array cell (a) Permittivity, (b) Permeability, and (c) Refractive Index

In the 2×2 array cell, the resonant frequency of 8.88 GHz, the permeability value is 156.85 and the permittivity value is 0.06. Similarly, the refractive index for 8.82 GHz and 8.87 GHz frequencies is 2.52 and 4.57. Figure 3.2-3 represents the surface current distribution of the (a) 1×2 array unit cell and (b) 2×2 array unit cell structure in the resonance frequency of 7.11 GHz to 8.86 GHz for the overall performance of the systems. The maximum magnitude of the proposed inverted L-C-shape unit cell is 193 Am^{-1}. From the concept of Maxwell's equation, the electric field and magnetic field are caused by the flow of charges or currents or by changing the field. Hence, in our research, an effective field performance and surface current distribution were observed in the proposed design carefully and obtained the required result. That provides a better data distribution policy. More than 4 times higher current distribution focused in 2×2 array unit cell structure is 716 Am^{-1}. In a 1×2 array unit cell, the surface current distribution is 151 Am^{-1}. Here, the surface current distribution pattern is represented in a 2D plane with a y-axis and an x-axis. Figure 3.2-5 indicates the direction of the electric field and magnetic field where the magnitude of the electric force is 2.33×10^5 Vm^{-1} and 653 Am^{-1} is the magnitude of the magnetic field. The maximum magnitude of the electric field and the magnetic field is 45549 Vm^{-1} and 183 Am^{-1} respectively, at the given frequency range from 6.5GHz to 9.5GHz. At 90^0 phase shift occurred in the array structure and the field direction.

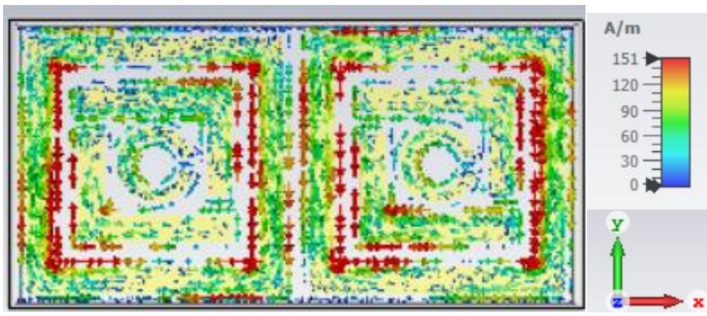

(a)

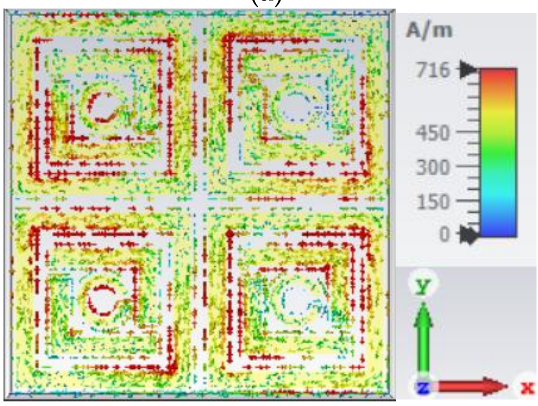

(b)

Fig 3.4-3: Surface Current Distribution at the operating frequency 7.11 GHz to 8.86 GHz (a) 1×2 array unit cell (b) 2×2 array unit cell

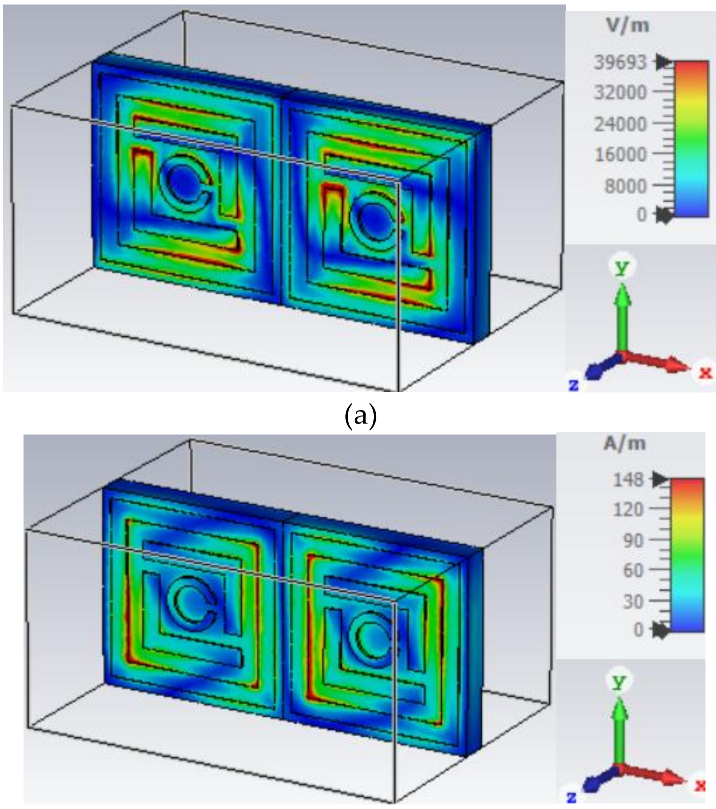

(b)

Figure 3.4-4: 1×2 Array Response of (a) Electric Field and (b) Magnetic Field

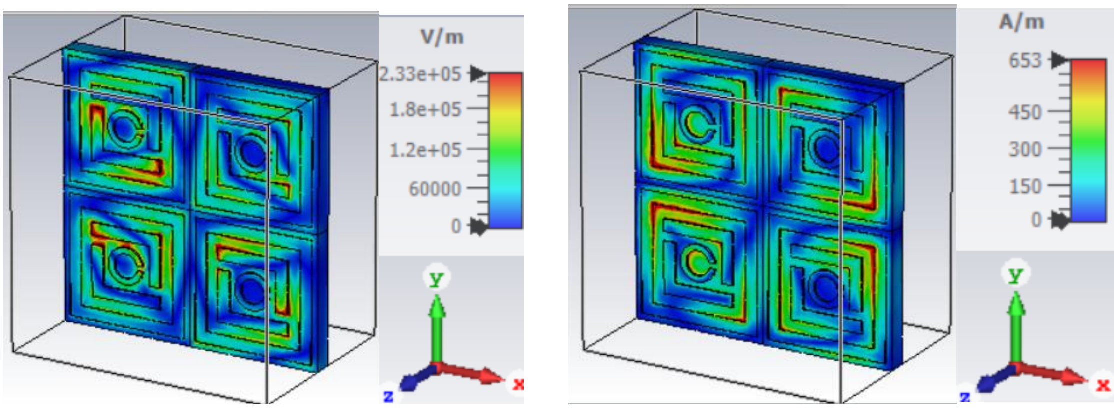

(a) (b)

Figure 3.4-5: 2×2 Array Response of (a) Electric Field and (b) Magnetic Field

3.5 COMPARISON BETWEEN PREVIOUS WORK AND PROPOSED UNIT CELL

Table 3.3-1 verifies previous studies and the proposed unit cell and metamaterials arrays from 6.5 GHz to 13.5 GHz frequency range. The proposed unit cell provides a better response when transmitting co-efficiently. Also, the characteristics of the epsilon negative and mu negative materials were observed in this design.

Table 3.3-1 The verification of some previous studies and the proposed unit cell and arrays of metamaterials

Ref. No.	**Shape of Unit cell**	**Size (mm^2)**	**Operating frequency (GHz)**	**Materials Type**	**Frequency Band**
[8]	Square SRR	12.3× 12.3	1.2-2.4	NRI	L
[10]	Z	10×10	2.0-14.0	LHM	C, X
[11]	Phi-shaped SRR	35×35	1.25-3.0	NRI	S
[12]	MDD-SRR shape	9×9	2.0-18.0	ENG	S, X, Ku
[13]	G-shape	22.5×22.5	2.0-4.0	NM	S
[14]	Coupled square and circle	23×23	0.5-2.0	NRI	L
[15]	RA	2.75× 2.75	30-50	NM	Ka
[16]	RIS	10×10	28-30	NM	Ka
Proposed design	Inverted L-C-shape	11×11	6.5-9.5	SNG (ENG)	C, X

NM=Not mentioned

Chapter 4: EBG ANTENNA DESIGN AND OPTIMIZATION

4.1 I-SHAPE MICROSTRIP PATCH ANTENNA DESIGN

4.1.1 Design Procedure

To originate the proposed Inverted L-C-shape electromagnetic band gap antenna, a 22×22 mm^2 dimension base conventional microstrip patch antenna was designed by a 50-ohm microstrip line feeding method in our proposed thesis work in Figure 4.1-1. So, to ensure the maximum power supply into the transmission line the impedance matching provides better radiation. Generally, the impedance (Z) of the patch is calculated by the following equation [46],

$$Z = 90\frac{{\varepsilon_r}^2}{\varepsilon_r - 1}(\frac{L}{W})^2 \qquad (10)$$

Where, ε_r indicates the dielectric constant of the substrate. Obtaining a proper antenna performance substrate choice is another important factor such as the FR-4 substrate used in this design. The dielectric constant of this substrate is $\varepsilon_r = 4.3$ and 1.6 mm in height(h) used in this design. The substrate and ground plane are both the same in dimension. However, the width (W) and length (L) of this patch are given by the following equations,

$$W = \frac{c}{2f_r}\sqrt{\frac{2}{\varepsilon_r + 1}} \qquad (11)$$

The speed of light indicated 'c' and f_r indicates the resonant frequency. In our design structure, the resonant frequency varies depending on the size or dimensions of the design. To obtain the actual length (L) of the patch refer to the difference in effective length (L_{eff}) and increasing length (ΔL) mentioned in equation (12) to (14). It occurs due to the unwanted magnetic and electronic field in the design so the effective dielectric constant (ε_{eff}) may be obtained from the following equation of (15)

$$L = L_{eff} - \Delta L \quad (12)$$

$$L_{eff} = \frac{c}{2f_r\sqrt{\varepsilon_{eff}}} \quad (13)$$

$$\Delta L = 0.412h\frac{(\varepsilon_{eff}+0.3)(\frac{W}{h}+0.264)}{(\varepsilon_{eff}+0.258)(\frac{W}{h}+0.8)} \quad (14)$$

$$\varepsilon_{eff} = \frac{\varepsilon_r+1}{2} + \frac{\varepsilon_r-1}{2}[1 + 12\frac{h}{W}]^{-1/2} \quad (15)$$

Hence, the height(h) of this substrate is 1.6 mm used in this design. According to the mentioned above equations [47] the overall structure of this proposed conventional designed. The metallic elements of copper(lossy) are used to cover the patch structure and ground plane. The width of 12.53 mm and the length of 9.9 mm copper are used for patch design with 0.035 mm thickness.

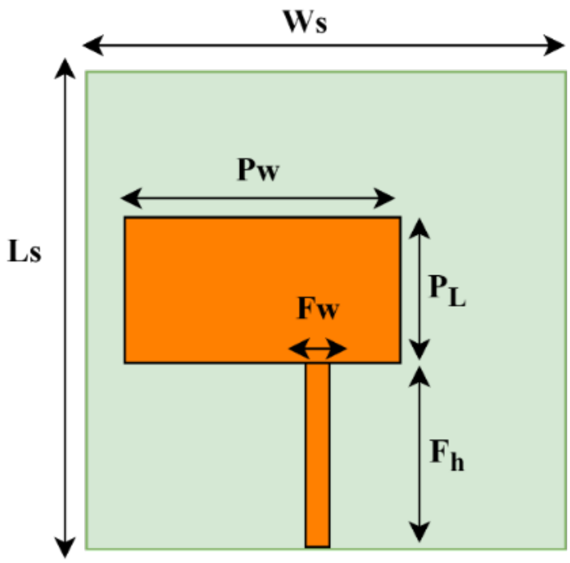

Fig 4.1-1: Geometrical Front Diagram of the proposed Rectangular Patch antenna

Here, the substrate is also replaced with Rogers RT5880 of 2.2 dielectric constants for multiple observations of the system. The overall system with port connection is solved by the time domain solver in CST Studio Suite 2021.Hexahedral mesh type solver setting used for simulation purpose. The C-band and X-band frequencies covered by this antenna performance at the resonant frequency of 7.11 GHz and 9.06 GHz respectively. The magnitude of S_{11} is -27.66 dB and -19.17

dB covered this required frequency band performance and other parameter performance (without EBG) presented in the result section.

4.1.2 Design Specification

Table 4.1-1 represents the measurement parameter list of the square patch antenna in mm scale.

Table 4.1-1: Parameter of the square patch antenna

Parameter List	**Dimensions(mm)**
Substrate Width, Ws	22
Patch Width, P_w	12.53
Width of Feed Line, F_w	0.125
Height of Feed Line, F_h	6.5
Patch Length, P_L	9.9
Substrate Length, Ls	22

4.2 PROPOSED EBG ANTENNA DESIGN

Figure 4.1-2 indicates the back view of the proposed inverted L-C-shape EBG antenna. The EBG unit cell applies the bottom of the ground plane. Different shapes are applied in this design. However, to load the proposed EBG structure first stage find out the transmission point of the selected plane corresponding to the wavelength (λ_0) in the antenna. To support the feeding line add the same transaction point as 50 ohm impedance matching. Perfect impedance matching provides perfect antenna radiation in Antenna technology. Here, the Plus shape of the design is applied also for modification purposes such as to detect the complicit of mutual coupling. P= 6.5 mm refers to the Half of the length in the y-axis and also q= 6.5 mm refers to the half of the length in the x-axis direction. The width of this entire Plus-shape is 0.50 mm. The ground plan also consists of 4.3 dielectric base copper metal with this unique EBG unit cell. The thickness is set as 0.035 mm. Four submissions of inverted L-C-shape EBG unit cell construct by the same dimension of Figure 4.2-1. To obtain good performance, substrate selection is a key factor for cost-effectiveness, low profile, and small size. FR-4 substrate and Rogers RT5880 substrate were used to observe the change in the desired outcomes. The dielectric constant of Rogers RT5880 is 2.2 and 4.3 is the dielectric constant of the FR-4 substrate. The thickness for these two substrates is the same, 1.6 mm. The return loss magnitude is -42.29 dB for the FR-4 substrate at the resonant frequency of 8.01 GHz which creates bandgap characteristics. At the resonant frequency of 7.49 GHz, the return loss is -13.26dB for the RT5880 substrate. Due to the size reduction of the patch dimension and proper impedance matching this EBG antenna is resonant at 8.01 GHz.

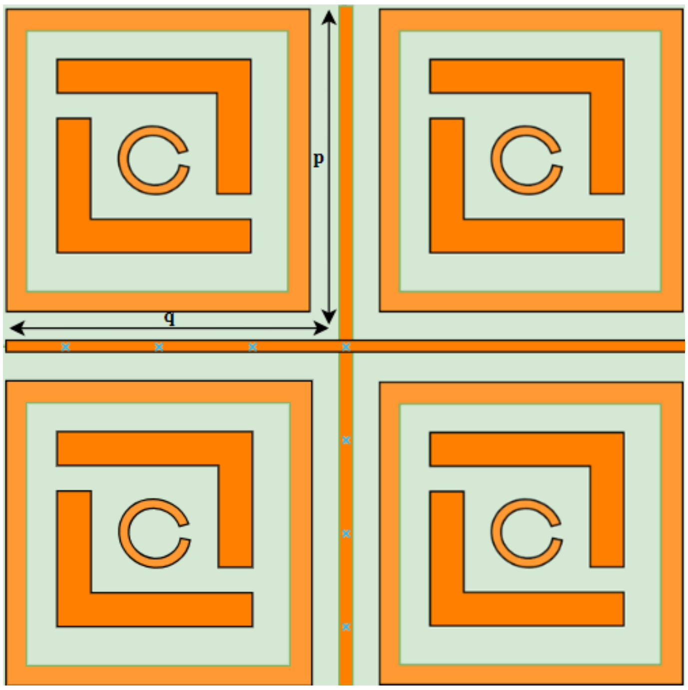

Fig 4.1-2: Back View of an Inverted L-C-shape EBG antenna

However, The C-band application was obtained by using the electromagnetic waves technique of our proposed EBG antenna design. It aslo offers lower band link of X-band frequency range so that the accuracy rate of propagation may obtain. Hence, To enhance the overall performance of antenna technology the concept of an EBG unit cell differs from other techniques and offers various types of applications in a certain frequency for any wireless communication system.

Chapter 5: RESULT ANALYSIS

5.1 ANALYSIS OF UNIT CELL AND ARRAY

To optimize the properties of the array unit cell the proposed inverted L-C-shape unit shape was developed in this work. So, the response of a unit cell is important to declare as a material. Hence, in our proposed unit cell design the maximum magnitude of transmission co-efficient (S21 = -70.44 dB) was obtained at the resonant frequency of 7.11 GHz in Figure 5.1-1. At the same operating frequency of 7.11 GHz, the 1×2 array cell responded to the magnitude of the transmission coefficient is -65.01 dB, and the 2×2 array cell provided a maximum magnitude of -68.39 dB.Fig.10 indicates the performance of the transmission coefficient for the proposed inverted L-C-shape unit cell, 1×2 array cell, and 2×2 array cell. Four resonance frequencies were obtained in an inverted L-C-shape unit cell design such as two resonant shifts created by electric resonance and the other two responses also created by the magnetic effect of the system. The C-band and X-band responses were observed in this performance of the proposed unit cell and also provided good observation in the communication system. Also, the higher bandwidth allows us to communicate a higher range of transmitting systems such as wideband communication systems. Similarly, Three-resonant frequencies were obtained in a 1×2 array cell structure. Due to the electric effect of this material, it provides two resonances at the frequency of 7.11 GHz and 7.82 GHz and covers the frequency band of C. From the 2×2 array cell, multiple resonance frequencies provide multiple responses of permittivity, permeability, and refractive index at the operating frequency from 6.5 GHz to 9.5 GHz. This array structure covered C-band, X-band, and Ku-band frequently and served a broader bandwidth in the communication sector. Fig.11 indicates the absorption rate of the proposed C-shape unit cell, 1×2 array cell, and 2×2 array cell. In Figure 5.1-2 , At the resonance frequency of 7.11 GHz, a 64% absorption rate was obtained in the designed 2×2 array cell which also reminds the capability of an absorber for broadband application. However, this proposed inverted L-C-shape unit cell and 1×2 array cell provide a maximum 45% and 53% absorption rate in this system. Hence, the performance of this proposed unit cell provides a wider range of bandwidth communication systems.

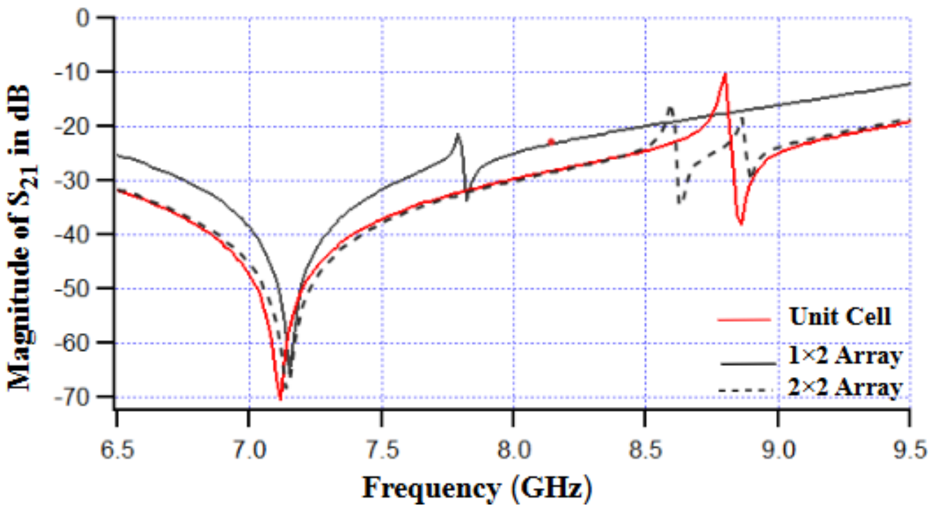

Fig 5.1-1: Performance of the magnitude of S21 with unit cell and array

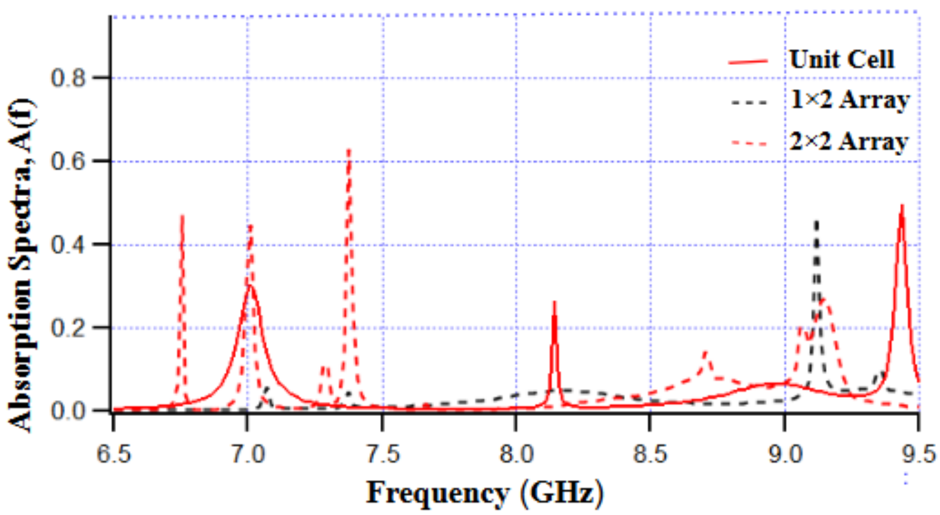

Fig 5.1-2: Response of absorption spectra (real part)

5.2 ANALYSIS OF EBG ANTENNA

Figure 5.2-1 represents the material analysis of the proposed Inverted L-C-shape EBG unit cell. In this graphical presentation, the resulting value of electric polarizability is ε = -1.69 at the resonant frequency of 7.11 GHz. The permeability(μ) is 483 at the resonant frequency of 7.11 GHz. At the same resonant frequency, the reflection index value is also positive such as n = 0.83. So, the resulting properties refer to the Epsilon Negative (ENG) Materials and cover the C-band frequency range. As the epsilon value is less than zero for ENG materials. Generally, The refractive index defines the ratio between the speed of light and the speed of material. In unit cell design, the refractive index depends on the permittivity and permeability of the materials. So this refractive index factor may assist the magnetic and electric field to create the electromagnetic waves also. However, permittivity (ε), permeability (μ), and refractive index (n) values are -0.06,8.82 and 3.03 at the resonant frequency of 8.86 GHz. When permittivity and permeability are both negative properties then it refers to double negative materials. But either permittivity or permeability in negative properties then it refers to single negative materials or SNG materials. In our study, the resulting resonant frequency envelops the C-band and X-band frequency categories. Also, the material types refer to Single Negative (SNG) Materials. Particularly, the negative of permittivity refers to Epsilon Negative Materials (ENG). The application of this study in various sections such as wireless communication systems. Specifically, the utilizing properties of electromagnetic waves of ENG materials also provides strengthening gain in EBG Antenna technology and that's the goal of our study. So for any type of communication or controlling system developed by these unique characteristics. The exploration of the return loss performance of our proposed study is represented in Figure 5.2-2. At the resonant frequency of 8.01 GHz, the return loss magnitude is -42.29 dB for the proposed EBG antenna and covers the C-band quality to communicate. It also holds the lower link of the X-band (8GHz-12GHz) range.Here, the band gap occurs from 7.95 GHz to 8.04 GHz frequency range. Using the RT-5880 substrate the return loss is -13.26 dB at the resonant frequency of 7.49 GHz which also encloses the C-band frequency.

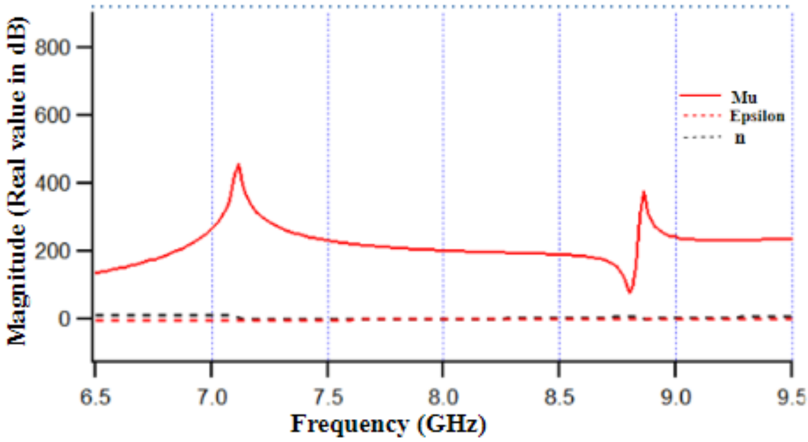

Fig 5.2-1: Analysis of ENG materials of the proposed Unit Cell

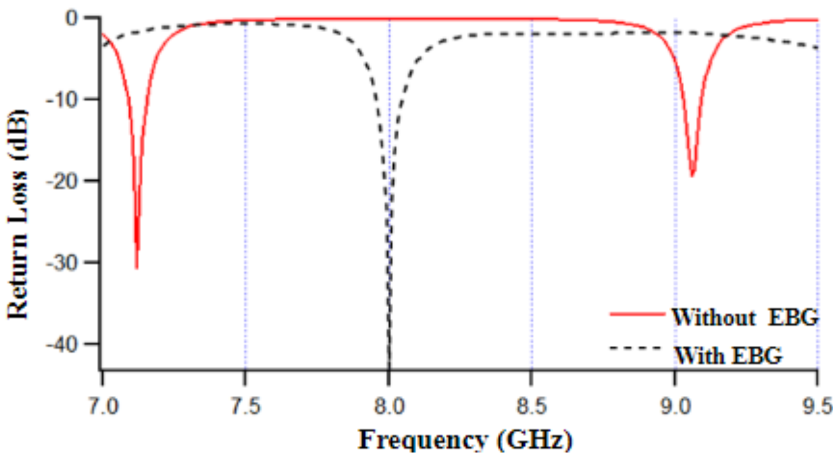

Fig 5.2-2: Return Loss Analysis of an Inverted L-C-shape EBG Antenna

On the other hand, the measurement of the reflected signal (S_{11}) of the patch antenna (without EBG) is -27.66 dB and -19.17 dB for the resonant frequencies 7.11 GHz and 9.06 GHz respectively. So the common band of C-band in conventional antenna and the proposed Inverted L-C-shape EBG antenna both are balanced and improve the systems. So, it reminds the better-reflated electromagnetic waves found without any disturbance in our proposed EBG design for its higher magnitude of return loss performance. Here, the desired bandwidth is covered by the frequency range 7.95 GHz to 8.04 GHz. A 90.0 MHz bandwidth was obtained from the inverted L-C-shape EBG antenna. Instead, the

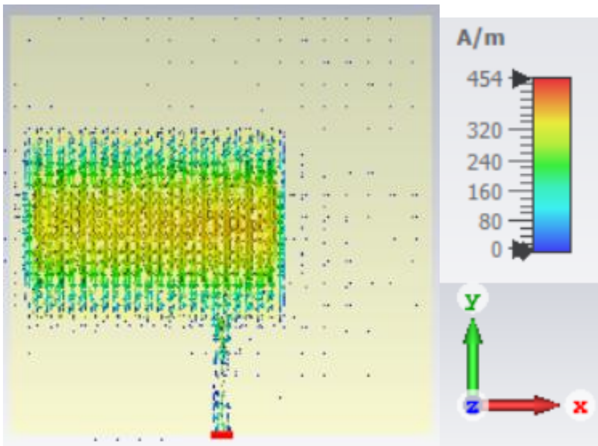

(a)

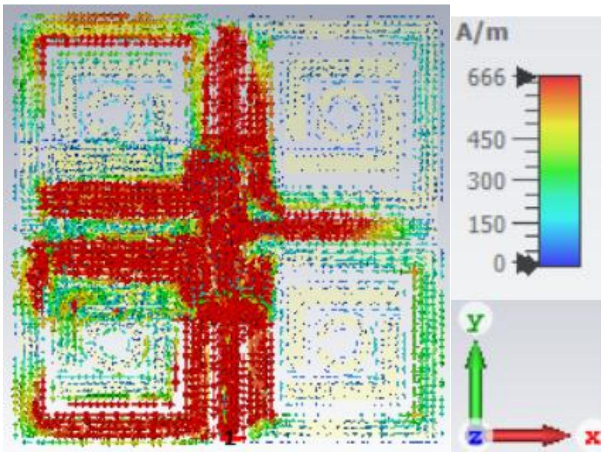

(b)

Fig 5.2-3: Surface Current Distribution (a) without EBG, (b) with EBG

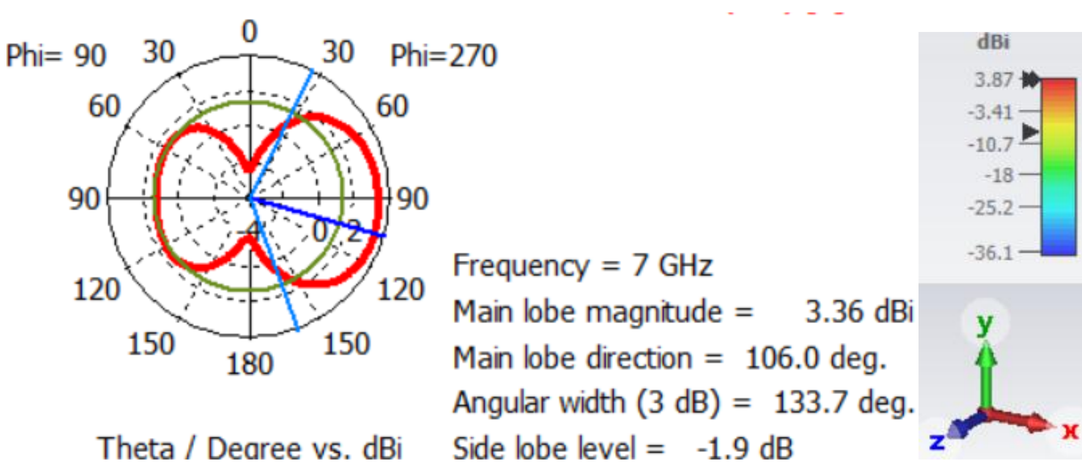

(a)

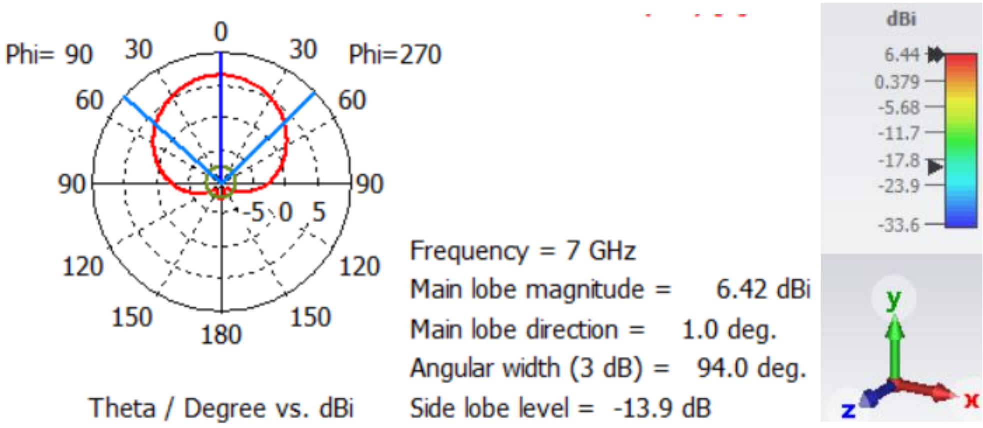

(b)

Fig 5.2-4: Gain of the proposed antenna (a) without EBG, (b) with EBG

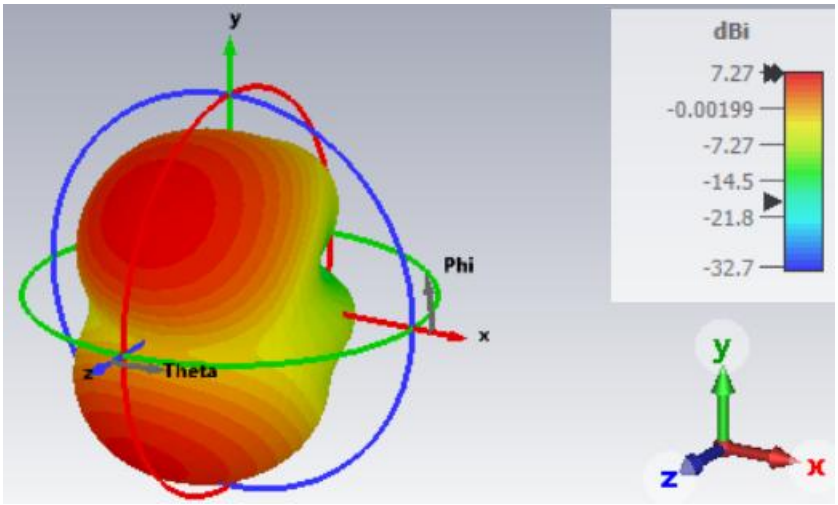

Fig 5.2-5: Directivity of the proposed EBG antenna

conventional microstrip patch antenna provides 60 MHz bandwidth and covers the frequency range from 7.09 GHz to 7.15 GHz. The efficiency rate is 68.52% which refers to good EBG antenna performance. Figure 5.2-3 focuses on the maximum magnitude of the current distribution is 454 Am^{-1} (without EBG) and 666 Am^{-1} (with EBG) at 90^0 angles. So, the flow of charges on the EBG antenna surface is higher than without the EBG structure. Figure 5.2-4 represents the gain of the antenna refer as a narrow high gain. The directivity of an antenna is equal to the ratio of the maximum power density to its average value over a sphere (Isotropic) as observed in the far field of an antenna. And gain is a realizable quantity that is less than directivity because of ohmic losses in the antenna. Here, the main lobe level magnitude is 6.42 dBi in our proposed EBG. Whereas, the far-field directivity is 7.27 dBi in the proposed EBG antenna design shown in Figure 5.2-5 at the angle of 90^0. Conversely, the proposed conventional patch antenna offers 4.48 dBi directivel So, an effective radiation pattern was obtained from this required design. So the resulting bandwidth from our study understood the higher bandwidth quality and return loss performance of the proposed EBG antenna than without the EBG antenna.

Chapter 6: CONCLUSIONS AND FUTURE WORK

6.1 CONCLUSIONS

The aim was to ensure that our proposed inverted L-C-shape ENG unit cell is in good condition to provide the performance of EBG antenna technology. So systematic materials or an effective EBG antenna design always supply goods application in the communication system without any trouble. In this study, a C-shape unit cell was also designed and optimized with good performance. Then 1×2 array unit cell and 2×2 array structure were observed. The unit cell and array provide the characteristics of ENG and MNG materials such as the material types also referred to as Single Negative (SNG) Materials. So the resulting properties refer to the Epsilon Negative (ENG) Materials and cover the C-band and X-band frequency range. Stepwise determination of transmission coefficient obtained in this proposed design. Also, the ability of an absorber observed very carefully depends on the magnitude of the wavelength of electromagnetic waves. At the resonant frequency of 8.01 GHz, the return loss magnitude is -42.29 dB with 6. 42 dBi gain and 7.27 dBi directivity for the proposed EBG antenna and covers the C-band quality to communicate. A 90.0 MHz bandwidth is obtained from the inverted L-C-shape EBG antenna. Instead, the conventional patch antenna provides 60 MHz bandwidth. Our proposed EBG Antenna ensures the enhanced quality of gain, directivity, and return loss performance at the required frequency of 8 GHz. Here, the proposed materials and EBG antenna both enclose the C-band frequency by the characteristics of electromagnetic waves.

6.2 FUTURE WORKS

However, The metamaterial may serve as an absorber or sensing application, clocking, filtering, and broadcasting all over the world. The EBG antenna may be used in high-power or high-speed circuits for data connection. Various types of applications are covered by the quality of a broader range of single or double frequencies in communication technology. Also, the limitation of the C-band or X-band frequency range may be overcome by the improvement of the properties of materials or antenna parameters. By using cost-effective instruments fabrication is possible. The analysis and applications of EBG structures may improve EBG antenna technology. Due to the effective installation process and propagation of the C-band and X-band range, the design may fabricated and also provides good performance in communication systems.

Bibliography

[1] Dina Serhal, Mohamad Hajj, Régis Chantalat, Julien Drouet and Bernard Jecko, "Multifed Sectoral EBG Antenna for WiMAX Applications", IEEE Antennas and Wireless Propagation Letter, vol. 8, 2009.

[2] F. Yang and Y. Rahmat-Samii, Electromagnetic Band Gap Structures in Antenna Engineering, Cambridge University Press Cambridge, UK, 2009.

[3] Ullah, M. H., Islam, M. T., & Faruque, M. R. I. (2013). A near-zero refractive index meta-surface structure for antenna performance improvement. *Materials*, *6*(11), 5058-5068.

[4] Smith, D. R., Padilla, W. J., Vier, D. C., Nemat-Nasser, S. C., & Schultz, S. (2000). Composite medium with simultaneously negative permeability and permittivity. *Physical review letters*, *84*(18), 4184.

[5] Li, L. W., Li, Y. N., Yeo, T. S., Mosig, J. R., & Martin, O. J. (2010). A broadband and high-gain metamaterial microstrip antenna. *Applied Physics Letters*, *96*(16).R. Nicole, "Title of paper with only first word capitalized," J. Name Stand. Abbrev., in press.

[6] Li, D., Szabó, Z., Qing, X., Li, E. P., & Chen, Z. N. (2012). A high gain antenna with an optimized metamaterial-inspired superstrate. *IEEE transactions on antennas and propagation*, *60*(12), 6018-6023.M. Young, The Technical Writer's Handbook. Mill Valley, CA: University Science, 1989.

[7] Ullah, M. H., Islam, M. T., & Faruque, M. R. I. (2013). A near-zero refractive index meta-surface structure for antenna performance improvement. *Materials*, *6*(11), 5058-5068.

[8] Zarghooni, B., Dadgarpour, A., & Denidni, T. A. (2015). Greek-key pattern as a miniaturized multiband metamaterial unit cell. *IEEE Antennas and Wireless Propagation Letters*, *14*, 1254-1257.

[9] Mishra, N., Choudhary, D. K., Chowdhury, R., Kumari, K., & Chaudhary, R. K. (2017). An investigation on compact ultra-thin triple band polarization-independent metamaterial absorber for microwave frequency applications. *IEEE Access*, *5*, 4370-4376.

[10] Devi, K. K. A., Hau, N. C., Chakrabarty, C. K., & Din, N. M. (2014). Enhancement of bandwidth and gain by using 3× 4 arrays of metamaterial-based patch antenna for RF energy harvesting at GSM 1800. *International Journal of Engineering Research*, *3*(10), 618-623.

[11] Afsar, M. S. U., Faruque, M. R. I., Khandaker, M. U., Alqahtani, A., & Bradley, D. A. (2022). A new compact split ring resonator based double inverse epsilon

shaped metamaterial for triple band satellite and Radar Communication. *Crystals*, *12*(4), 520.

[12] M. M. Hasan, M. R. I. Faruque, S. S. Islam, and M. T. Islam, "A new compact double-negative miniaturized metamaterial for wideband operation," Materials (Basel)., vol. 9, no. 10, pp. 1–12, 2016, doi: 10.3390/ma9100830.

[13] Saravanan, M., & Umarani, S. M. (2018). Gain enhancement of patch antenna integrated with metamaterial-inspired superstrate. *Journal of Electrical Systems and Information Technology*, *5*(3), 263-270.

[14] Hossain, M. J., Faruque, M. R. I., & Islam, M. T. (2017). Design and analysis of a new composite double negative metamaterial for multi-band communication. *Current Applied Physics*, *17*(7), 931-939.

[15] Suzuki, T., & Asada, H. (2020). Reflectionless zero refractive index metasurface in the terahertz waveband. *Optics Express*, *28*(15), 21509-21521.J. Clerk Maxwell, A Treatise on Electricity and Magnetism, 3rd ed., vol. 2. Oxford: Clarendon, 1892, pp.68–73.

[16] Advancements in Mobile Communication: A Novel Sectoral Antenna Design Incorporating Magneto-Electric Curved Strip Dipoles and PRS Superstrate January 2024 IEEE Access PP(99):1-1

[17] Krishnananda, K., & S Rukmini, T. (2012). EBG antennas: Their design and performance analysis for wireless applications. *International Journal of Computer Applications*, *48*(23), 20-27.

[18] Yarga, S., Sertel, K., & Volakis, J. L. (2008). Degenerate band edge crystals for directive antennas. *IEEE transactions on antennas and propagation*, *56*(1), 119-126.

[19] Dewan, R., Rahim, M. K. A., Himdi, M., Hamid, M. R., Majid, H. A., & Jalil, M. E. (2017). Multiband frequency-reconfigurable antenna using metamaterial structure of electromagnetic band gap. *Applied Physics A*, *123*, 1-7.

[20] J. S. Colburn and Y. Rahmat-Samii, "Patch antennas on externally perforated high dielectric constant substrates," IEEE Trans. On Antennas and Propagation, vol. 47, no. 12, pp. 1785-1794, 1999.

[21] Said, S., Es-salhi, A., Abdelmoumen, K., & Elouaham, S. (2022). New integrated dual-band dipole antenna with EBG structures designed for wireless communications. *International Journal of Electrical and Electronic Engineering and Telecommunications*, 184-191.

[22] Faruque, M.R.I.; Islam, M.T.; Misran, N. Design analysis of new metamaterial for EM absorption reduction. Prog. Electromagn. Res. 2012, 124, 119–135.

[23] Islam, S. S., Faruque, M. R. I., & Islam, M. T. (2014). The design and analysis of a novel split-H-shaped metamaterial for multi-band microwave applications. *Materials*, *7*(7), 4994-5011.

[24] Wasel, H., & Guoping, Z. (2018). Enhancing 5G patch array antenna gain using

DNG metamaterial. *International Journal of Energy Engineering*, *8*(4), 93-96.

[25] Zhang, Xiaoyan, et al. "Design of a Reconfigurable Band-notched Wideband Antenna using EBG Structures." *The Applied Computational Electromagnetics Society Journal (ACES)* (2023): 895-902.

[26] Kaabal, A., El Jaafari, B., Ahyoud, S., & Asselman, A. (2018). Design of EBG antenna with multi-sources excitation for high directivity applications. *Procedia Manufacturing*, *22*, 598-604.

[27] Zi-Jian Han, Wei Song, Wen-Ji Li, and Xin-Qing Sheng, "High-gain and low-profile ebg patch antenna design," *2016 Progress in Electromagnetic Research Symposium (PIERS)*, Shanghai, 2016, pp. 1676-1679, doi: 10.1109/PIERS.2016.7734759.

[28] Raut, H., Kingsly, S., Subbaraj, S., & Malekar, R. (2024). EBG-based slotted T-shaped antenna for sub-6 GHz 5G application. *International Journal of Electronics Letters*, 1-13.

[29] Djoudi, M., Tounsi, M. L., & Yagoub, M. C. (2024). Efficient Design of a 2D EBG Circular Microstrip Antenna for 5G Applications. *AIJR Abstracts*, 49-50.

[30] Kushwaha, N., & Kumar, R. (2014). Study of different shape electromagnetic band gap (EBG) structures for single and dual band applications. *Journal of Microwaves, Optoelectronics and Electromagnetic Applications*, *13*, 16-30.

[31] Yazdi, M., & Komjani, N. (2011). Design of a band-notched UWB monopole antenna by means of an EBG structure. *IEEE Antennas and Wireless Propagation Letters*, *10*, 170-173.

[32] S. Sara and E. -S. Abdenacer, "Novel Dual-Band Dipole Antenna Integrated with EBG Electromagnetic Bandgap Structures Dedicated to Mobile Communications," *2019 International Conference on Wireless Technologies, Embedded and Intelligent Systems (WITS)*, Fez, Morocco, 2019, pp. 1-5, doi: 10.1109/WITS.2019.8723660.

[33] Singh, D., Thakur, A., & Srivastava, V. M. (2018). Miniaturization and Gain Enhancement of Microstrip Patch Antenna Using Defected Ground with EBG. *J. Commun.*, *13*(12), 730-736.

[34] Saha, D., & Saha, C. (2022, December). MTM-EBG Loaded Circular Patch Antenna for ISM Band Applications. In *2022 IEEE Microwaves, Antennas, and Propagation Conference (MAPCON)* (pp. 1788-1791). IEEE.

[35] Dam, T. H., Le, M. T., Nguyen, Q. C., & Nguyen, T. T. (2023). Dual-Band Metamaterial-Based EBG Antenna for Wearable Wireless Devices. *International Journal of RF and Microwave Computer-Aided Engineering*, *2023*(1), 2232674.

[36] Abdulhamid, M., Rahim, M. K. A., & Musa, U. (2015). Electromagnetic bandgap structure for antenna design. *IOSR J Electron Commun Eng*, *10*(06), 25-27.

[37] Riadi, S., Triono, S., Syahril, S., & Nofriansyah, D. (2019). Effectiveness of Metacognitive Learning's Model in Engineering. *International Journal of*

Engineering and Advanced Technology (IJEAT), *9*(1), 4438-4443.

[38] Tlili, B. (2010, July). Design of double C-slot microstrip patch antenna for WiMax application. In *2010 IEEE Antennas and Propagation Society International Symposium* (pp. 1-4). IEEE.

[39] Latha, S., & Anand, P. R. (2016, March). Circular polarized microstrip patch array antenna for wireless LAN applications. In *2016 International Conference on Wireless Communications, Signal Processing and Networking (WiSPNET)* (pp. 1197-1200). IEEE.

[40] Shajahan, S., & Lethakumary, B. (2014, July). Wideband microstrip array antenna using Electromagnetic Band Gap structures. In *2014 Annual International Conference on Emerging Research Areas: Magnetics, Machines and Drives (AICERA/iCMMD)* (pp. 1-5). IEEE.

[41] Díaz, A. M. S., Galaz-Larios, M. C., & Ramírez-García, E. (2017, August). Analysis and design of electromagnetic band gap structures with application in planar antennas. In *2017 42nd International Conference on Infrared, Millimeter, and Terahertz Waves (IRMMW-THz)* (pp. 1-2). IEEE.

[43] Almutairi, A. F., Islam, M. S., Samsuzzaman, M., Islam, M. T., Misran, N., & Islam, M. T. (2019). A complementary split ring resonator based metamaterial with effective medium ratio for C-band microwave applications. *Results in Physics*, *15*, 102675.

[44] Pendry, J. B. (2000). Negative refraction makes a perfect lens. *Physical review letters*, *85*(18), 3966.

[45] Islam, S. S., Faruque, M. R. I., & Islam, M. T. (2015). A new direct retrieval method of refractive index for the metamaterial. *Current Science*, 337-342.

[46] Alsager, A. F. (2011). Design and analysis of microstrip patch antenna arrays. *Unpublished Masters Thesis, University College of Boras, Sweden*, *1*, 1-80.

[47] Inum, R., Rana, M. M., & Quader, M. A. (2016, September). Modeling of an efficient microstrip patch antenna for microwave brain imaging system. In *2016 3rd International Conference on Electrical Engineering and Information Communication Technology (ICEEICT) (pp. 1-6). IEEE.*

[48] Mishra, S., & Satpathy, S. (2003). One-dimensional photonic crystal: The Kronig-Penney model. *Physical Review B*, *68*(4), 045121.

[49] CST Microwave Studio– Solve & Overview, CST Studio Suit 2010, CST-Computer Simulation Technology AG, Internet site address: http://www.cst.com.